4. Soil-Water Relationships in Saline and Alkali Conditions

Water as solvent, reactant and transporting agent plays an important (sometimes decisive) role in weathering and soil formation processes, in the mass and energy transport and/or transformation of soils and consequently, in the development of potential and actual soil fertility [GARDNER 1960; HADAS 1973; HILLEL 1972; KOVDA 1974; NERPIN and CHUDNOVSKY 1975; RIJTEMA 1968; VÁRALLYAY 1977, 1978a, 1978b, 1978c, 1978d]. The genesis of various soil categories, the formation of their diagnostic horizons and their characteristic physical, chemical, biological and agronomical properties are also related to soil water, since the soluble compounds (and sometimes insoluble materials such as organic and inorganic colloids, clay particles, etc.) move with the water; there is a permanent interaction between the solid and liquid phases of the soils [KUTILEK 1973; SZABOLCS 1969, 1974; DARAB 1974; DARAB and RÉDLY 1967]; and soil water strongly influences the biological processes. The quantity, state (availability) and movement of the soil water determine the water supply of natural plants and cultivated crops, and indirectly regulate their nutrient uptake and metabolism, as well. Consequently, the soil moisture regime has special significance among soil ecological factors, influencing (sometimes determining) the ecological potential of a given area, the biological productivity, i.e. the biomass production of various natural and agricultural ecosystems [HADAS 1973; HILLEL 1972; KOVDA 1974; RUSSEL 1973].

Salinity and alkalinity are important phenomena in the biosphere: they limit soil fertility, impede soil utilization and prevent intensive agricultural development.The distribution of the present salt affected soils is closely related to climatical, geological, geochemical, hydrological and hydrogeological conditions. These soils raise serious problems in numerous countries, especially in arid and semi-arid regions of the World, not only regarding the natural environment but in respect of the national economy as well [GARDNER 1960; International Source Book 1967; Proc. Symp. ISSS Subcomm. 1965, 1969, 1975; WORTHINGTON 1977; VÁRALLYAY 1977, 1978b].

The primary reason for the formation and occurrence of salt affected soils is the accumulation of Na^+ ions in the solid and/or liquid phase of the soils [SZABOLCS 1969, 1974; KOVDA 1947]. Consequently, soil-water plays a decisive role in the development of salt affected soils, in the salinization and alkalization processes: the soluble salts are transported by water and according to the solid-liquid interface phenomena (cation exchange, miscible displacement, etc.) the chemical characteristics (concentration, ion composition) of the soil solution governs the exchangeable ion composition of the soil absorption complex and the properties of solid soil constituents [DARAB 1974;

KOVDA 1947; SZABOLCS 1969, 1974; YONG and WARKENTIN 1975]. This influences the

— mineralogical status (degradation, destruction and formation of clay minerals, orientation of clay particles, etc.);

— rate of hydration and dispersion;

— swelling-shrinkage-cracking phenomena;

— arrangement of primary particles, shape, size and stability of soil micro- and macro-aggregates, structural elements, consequently the pore-size distribution;

— factors of soil moisture regime: spatial (vertical and horizontal) and time distribution of moisture content, moisture potential and moisture movement (vapour transfer, saturated and unsaturated flow) [GARDNER 1960; HADAS et al. 1973; International Source Book 1967; KUTILEK 1973; MCNEAL et al. 1968; NIELSEN 1972; VÁRALLYAY 1972, 1974c, 1976a, 1976b, 1977, 1978b; WIT and KEULEN 1972].

The interactions between heavy-textured swelling clays and alkaline sodium-salt solutions are particularly significant and result in radical changes in the water economy of the soil and consequently in mass and energy transport and transformation, thus creating a special and extreme soil ecological environment for native vegetation or agricultural crops [HILLEL 1972; International Source Book 1967; KOVDA 1974; RUSSEL 1973].

In many cases the fertility and agricultural utility of salt affected soils are limited mainly by their unfavourable physical properties and extreme water economy [GARDNER 1960; HILLEL 1972; Proc. Symp. ISSS Subcomm. 1965, 1969, 1975; VÁRALLYAY 1977, 1978b, 1978c; VÁRALLYAY and SZABOLCS 1974, 1978].

The main soil factors limiting the optimum (adequate and continuous) water supply of plants are schematically illustrated in Figures 4.1, 4.2 and 4.3 [VÁRALLYAY 1978c].

In Figure 4.1 the main causes and consequences of the limited water storage capacity of soils are summarized. In coarse-textured soils (coarse sands, humous sands, etc.) the limited water storage capacity (FC) is mainly due to the limited water retention, the extremely high infiltration rate (IR) and hydraulic conductivity (HC). These are the main reasons for the low fertility and extreme drought sensitivity of these soils.

In the case of a surface crust (cemented by Na-salts, gypsum, $CaCO_3$, etc. or compacted by misguided soil management) or a compact soil layer (various hardpans; horizons cemented and compacted by the accumulation of inorganic colloids, clay, exchangeable Na^+, etc.) near to the surface, not only the root penetration is retarded, but the infiltration of water into the soil is also limited and creates an extreme moisture regime. The very low infiltration rate results in oversaturation and aeration problems (decreasing availability of plant nutrients, anaerobic biological processes, unfavourable reduction phenomena, etc.) in the shallow wetting zone, in temporary water-logging after rainfall or irrigation and in considerable evaporation losses and surface runoff (→ lateral erosion). The water storage capacity of this shallow wetting zone is very low: thus it can only satisfy the water consumption of the plants for a short period. This is the main reason for the special drought sensitivity of heavy-textured alkali soils even under irrigated conditions (Fig. 4.1).

Crack formation in swelling clays causes another water problem in heavy-

textured alkali soils (Fig. 4.2). When the soil is dry, some of the rain or irrigation water flows through the open cracks directly into the ground water. These "filtration losses" diminish the water storage in the soil, decrease water use efficiency and, at the same time, may result in a rise in the water table, which may be accompanied by such unfavourable processes as water-logging, over-

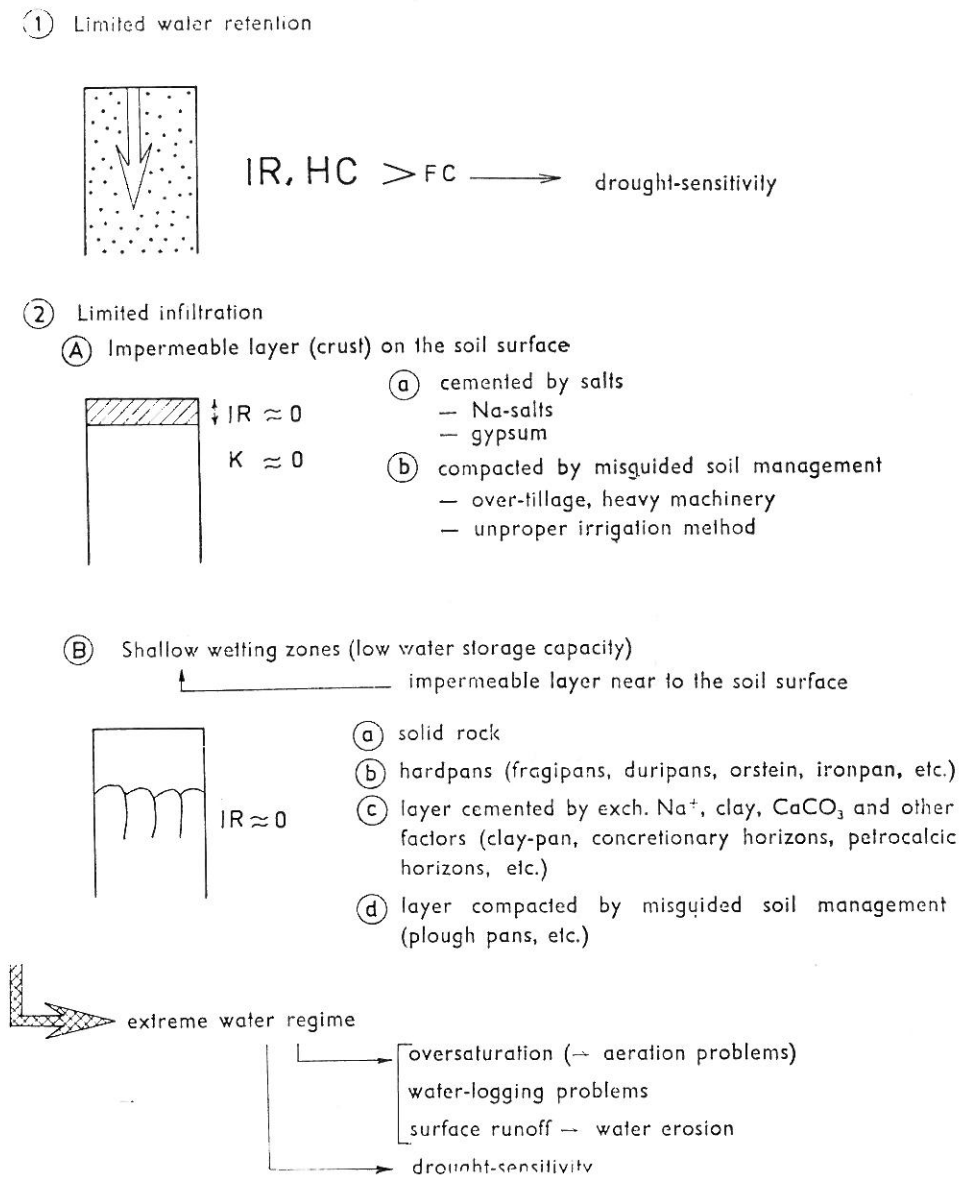

Fig. 4.1
Soil factors limiting optimum water supply of plants. I. Limited water storage capacity

saturation (in the case of a high water table) or secondary salinization and alkalization (in the case of a shallow, stagnant, saline ground water). During dry periods the soil may dry out deeply through the deep and wide cracks (causing considerable evaporation losses). In rainy seasons the clogging cracks impede the uniform wetting of the soil and result in problems similar to those found in impermeable soils.

A further group of soil factors limiting the optimum water supply of plants can be summarized as "low availability" of soil moisture (Fig. 4.3). It is the direct or indirect consequence of various phenomena:

— narrow available moisture range (AMR) in coarse-textured soils because of their very low water retention (low field capacity, FC);

— narrow AMR in heavy-textured (sometimes Na^+-saturated) swelling clays because of their very high water retention (high wilting percentage, WP);

— high osmotic potential (ψ_s) due to the high concentration of the soil solution (in comparison with the electrolyte concentration in the plant root tissues);

— extremely low transport coefficients (capillary conductivity, k, and diffusivity, D); in spite of the high suction gradient the flux from the wet soil to the plant roots is extremely slow through the thin but rather dry "film-

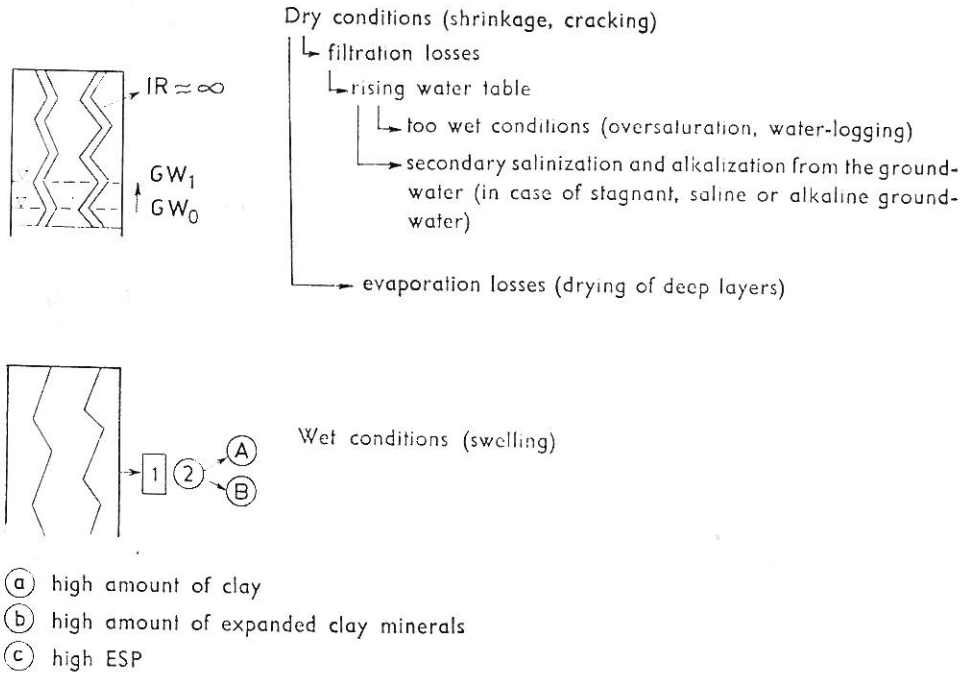

Fig. 4.2
Soil factors limiting optimum water supply of plants. II. Cracking (swelling-shrinkage phenomena)

like" moisture depletion zone formed around the plant roots. As a consequence of this peculiar microdistribution pattern of soil moisture, the adequate water supply of the plants (especially of crops with widely-spaced and scarce root-systems) is limited and they show water deficiency symptoms even if the soil bulk has considerable moisture content [ARYA 1973; HADAS et al. 1973; KUTILEK 1973; VÁRALLYAY 1976a, 1977, 1978b, 1978c].

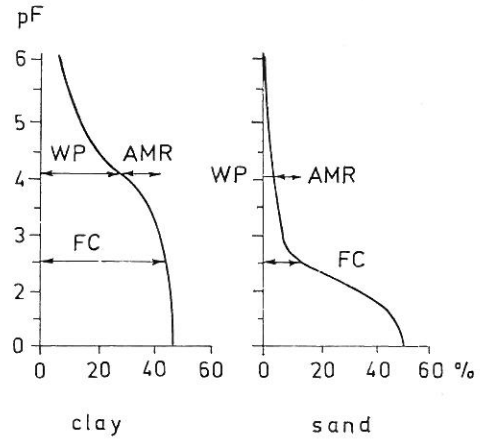

① Low AMR (FC — WP)

as a result of matrix suction (Ψ)

ⓐ high clay content
ⓑ high rate of dispersion
ⓒ high alkalinity, ESP
ⓓ poor structure
ⓔ too low clay content

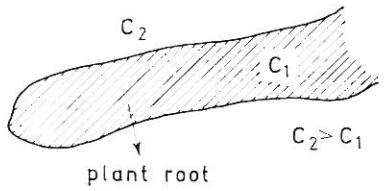

② Low AMR

as a result of high osmotic potential (Ψ)

ⓐ high salinity

$\Psi_s = 0.32\ (0.8 + 0.109\ C_i)^{1.03}$

C_i = Cl^- conc. meq/lit.

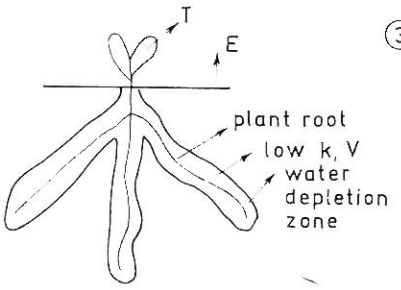

③ Low transmissability coefficients (k, D)

wilting: V < ET

ⓐ low moisture content
ⓑ high water retention
ⓒ high alkalinity, ESP
ⓓ poor structure

Fig. 4.3
Soil factors limiting optimum water supply of plants. III. Low availability of soil moisture

It can be concluded from the above mentioned facts that the exact description, prediction and quantitative characterization of moisture state and flow phenomena are of paramount importance in the study of salinization and alkalization processes, in the genesis, formation and evolution of salt affected soils, and from the viewpoint of their rational agricultural utilization and amelioration.

An efficient salinity and alkalinity control is possible only if the salt sources are determined; vertical and horizontal water and salt movements are exactly and quantitatively described; the influencing factors, their mechanisms and relationships are quantitatively analysed; salinization and alkalization processes are predicted [Prognosis of salinity and alkalinity, FAO Soils Bulletin 1976; SZABOLCS, DARAB and VÁRALLYAY 1969, 1972, 1976]. In regions where the ground water is the main salt source and subsurface waters play a decisive role in the development of salt affected soils, the salt accumulation processes from the ground water have primary importance. For the exact description and prediction of these processes various aspects have to be taken into consideration:

1. Meteorological aspect: time and territorial distribution of precipitation, potential and actual evapotranspiration, as the primary causes of suction gradient and water movement in soil.

2. Hydrogeological aspect: depth and fluctuation of water table, horizontal flow of ground water, etc.

3. Hydrophysical aspect: time and territorial distribution of moisture and suction profiles, water movement in the unsaturated soil layers and soil properties influencing these phenomena.

4. Chemical and physico-chemical aspect: time and territorial distribution of concentration and chemical composition of ground water and soil solution; the direct or indirect effects of these factors on the hydrophysical parameters; interactions between the solid and liquid phase of soils; etc.

When adequate data on these aspects are available the integrated analysis of the above mentioned factors can be carried out by multi-factorial mathematical models (with the use of computers) requiring well coordinated international cooperation [FRISSEL and REININGER 1974; HILLEL 1977; NERPIN and HLOPOTENKOV 1971; NIELSEN 1972; OLSZTA 1978; PACHEPSKY et al. 1976; SOKOLENKO et al. 1976; TYURYUKANOV and GALICKY 1976; WIT and KEULEN 1972].

4.1. Salinity-alkalinity and moisture status

Soil moisture status can be characterized by three factors:
- moisture content (including its spatial and time distribution);
- phase of soil water (ice, liquid, vapour);
- moisture potential (moisture retention, "availability").

The moisture content depends on external factors (climatic conditions: rainfall, evaporation, etc.; hydrological conditions: depth and fluctuation of water table, surface runoff, etc.; human activity: irrigation, drainage, land use, agrotechnics, etc.) and soil properties influencing the moisture transport (see below).

Any complete analysis and/or modelling of moisture equilibrium or flow problems requires the relations between water potential and the moisture (or

liquid) content of the soil to be known [BEAR, ZASLAVSKY and IRMAY 1968; GLOBUS 1969; KOVÁCS 1976; MICHURIN 1975; NERPIN and CHUDNOVSKY 1967, 1975; NIELSEN 1972].

At equilibrium, the constituent water of the liquid phase is subject to the action of the gravitational field, the influence of dissolved salts and of the solid phase (including adsorbed ions) in its given geometry of packing, and to the action of the local pressure in the soil gas phase. Together these factors determine the value of the total potential, ψ_t.

The total potential, ψ_t, of the constituent water in soil at temperature T_0, is the amount of useful work per unit mass of pure water, in J/kg, that must be done by means of externally applied forces to transfer reversibly and isothermally an infinitesimal amount of water from the standard state S_0 to the soil liquid phase at the point under consideration [Bull. ISSS 1976].

The components of the total potential (ψ_t) are:

$$\psi_t = \psi_g + \psi_s + \psi_p \tag{4.1}$$

where ψ_g = gravitational potential
ψ_s = osmotic potential
ψ_p = tensiometer-pressure potential.

The subcomponents of the tensiometer-pressure potential (ψ_p) are:

$$\psi_p = \psi + \psi_p^a \tag{4.2}$$

where ψ = matric potential
ψ_p^a = pneumatic potential.

The gravitational potential (ψ_g) and the pneumatic potential (ψ_p^a) are independent of the soil properties and from the salinity-alkalinity status of the soil. The osmotic potential (ψ_s) is a function of the concentration and ion composition of the soil solution; it can be directly measured by an osmometer and may be expressed in terms of the experimentally accessible osmotic pressure of the solution, π, according to the following equation:

$$\psi_s = -\int_0^{\pi} \bar{V}_w \, dP \tag{4.3}$$

in which $\bar{V}_w$ is the partial specific volume of the constituent water in the soil solution [Bull ISSS. 1976].

The osmotic soil water potential (ψ_s) can be computed for various soil solutions, e.g. for chloride type salinization it may be described by the following equation:

$$\psi_s = 0.32 \quad (0.8 + 0.109C_t)^{1.08} \tag{4.4}$$

where C_t represents the Cl^- concentration of the soil solution in me/l [HADAS et al. 1973; International Source Book 1967].

It is quite obvious that osmotic potential can limit or completely prevent the water uptake by the plant if

$$\psi_{ss} \geq \psi_{sr}$$

where ψ_{ss} = osmotic potential in soil solution
ψ_{sr} = osmotic potential in plant root tissue.

ψ_{ss} is high in saline soils, especially in soils with NaCl-Na_2SO_4 type salinization, because here, during drying, the concentration of the soil solution sharply increases (i.e. high solubility). In the case of $NaHCO_3$-Na_2CO_3 type salt accumulation, this sharp increase is limited by the lower solubility constants and therefore ψ_{ss} remains relatively lower. ψ_{sr} is a specific characteristic of the various plants and in extreme cases (in salt tolerant halophytic plants) it can be as high as 50—100 atm. [International Source Book 1967; HADAS et al. 1973; RUSSEL 1973].

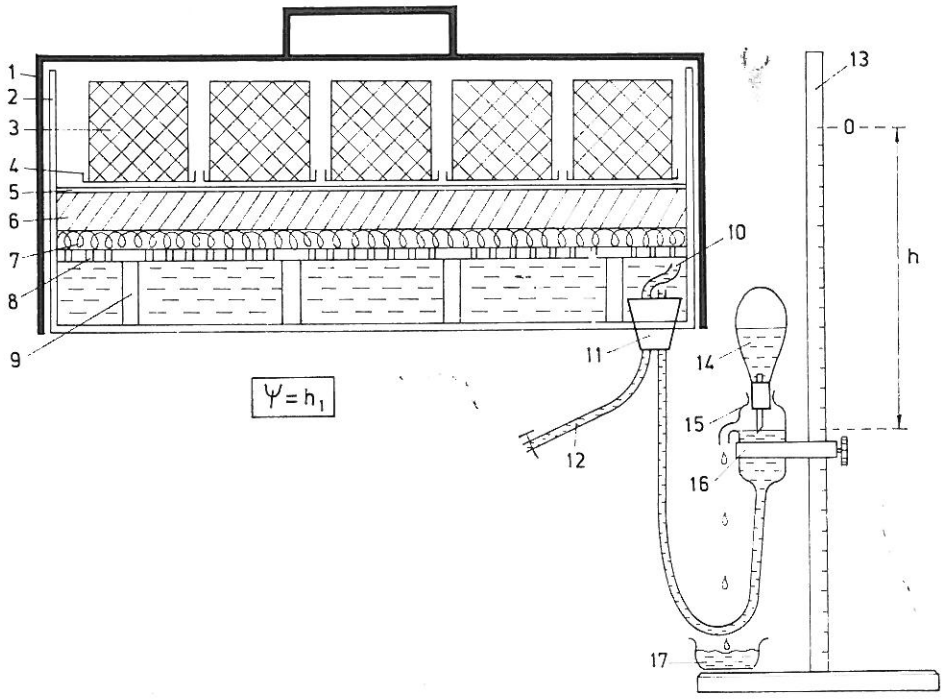

Fig. 4.4
Sand box apparatus for the determination of soil moisture retention curves in the suction range pF 0 to 2.0. 1. Non transparent PVC lid with lifting handle. 2. Plexi box, prepared from 9 mm thick transparent plexi plate. 3. Soil sample in brass or stainless steel cylinder numbered for identification (height 50 mm, volume 100 cm^3). 4. Nylon cloth attached to the lower opening of the cylinder using a rubber band. 5. Nylon cloth on the smooth surface of the porous medium. 6. Porous media: 2 cm thick coarse sand (air bubbling value $\psi_a = 40—50$ cm) layer for the determination of pF 1.0; 2—3 cm thick fine sand (air bubbling value $\psi_a = 140—150$ cm) layer for the determination of pF 1.5 and 2.0. 7. About 15 mm thick asbestos-wool layer. 8. 10 mm thick transparent plexi plate, perforated with pin holes of 4 mm diameter, spaced at 10×10 mm. 9. 25 mm transparent plexi legs of 13×13 mm sectional surface, spaced at 100×100 mm. 10. Glass tube used to remove air bubbles from the vacuum chamber filled with water. 11. Rubber stopper with two holes. 12. Transparent plastic-tubing with stopcock — for connection to the vacuum source (connected with the glass tube 10 used to remove air bubbles from the vacuum chamber). 13. Stainless steel sliding measuring stand with cm graduation. 14. Levelling (supply) bottle. 15. Constant-level bottle with overflow tube. 16. Clamp supporting the constant-level bottle, can be moved and fixed with a wing-screw. 17. Collecting vessel

The matric potential (ψ) expresses the vectorial sum of various attractive forces connected with the solid phase of the soil, i.e. the soil matrix (capillary forces, sorptive forces, etc.). Consequently, in most cases the state and "availability" of soil moisture are mainly determined by ψ (isothermal conditions, low salinity, etc.). Therefore pF-curves (suction—moisture content relationships) have special significance in the exact and quantitative characterization of the soil moisture status and the hydrophysical properties of soils.

pF curves clearly reflect the quantity of soil moisture bound by various attractive forces and the ratio between the air-filled and water-filled pores in the unsaturated soil layers under a given suction. Consequently, they can be used [VÁRALLYAY 1973a]:

— for the exact characterization of soil moisture potential and the energy-state of the liquid phase of the soil;

— for the quantitative characterization of physical and hydrophysical properties of soils and their moisture regime and the classification and mapping of soils according to their water management;

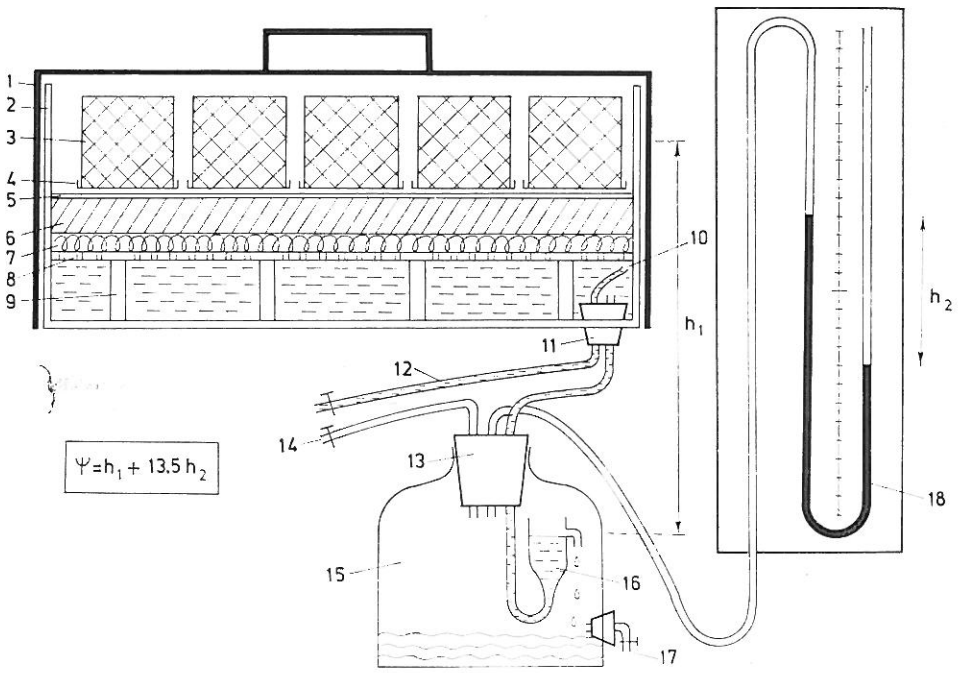

Fig. 4.5

Kaolin box apparatus for the determination of soil moisture retention curves in the suction range pF 2.0 to 2.7. 1—12 as in Figure 4.4. The porous medium in this apparatus is a mixture of fine sand and kaolin (air bubbling value $\psi_a = 600-700$ cm). For the determination of pF 2.3 a 2.5—3.5 cm thick layer of 2 : 1 fine sand — kaolin mixture, for the determination of pF 2.7 a 4—5 cm thick layer of 1 : 1 fine sand—kaolin mixture. 13. Rubber stopper with three holes. 14. Vacuum tube for connection to the vacuum stabilizer (automatic mercury stabilizer). 15. Collecting bottle and at the same time depression vessel: thick-walled 10—15 litre glass bottle. 16. Constant level vessel. 17. Stopcock to drain the accumulated water. 18. Mercury manometer

— for the estimative characterization of pore-size distribution in soils (mostly in sands);

— for the determination of soil moisture constants such as:

— total porosity (P_T), total water capacity (TC) = pF 0;

— field capacity (FC) = pF 2.0—2.7;

— wilting percentage (WP) = pF 4.2;

— hygroscopicity (hy) = pF 6.2;

— available moisture range (AMR) = FC—WP.

— for the registration and monitoring of changes in the physical and hydrophysical properties of the soil due to natural factors or induced by human activities;

— in irrigation practice: for the scheduling of irrigation; the determination of the optimum (or ecologically and economically rational) frequency of irrigation; the dose of irrigation water required and which can be applied without any harmful side-effects; the selection of proper irrigation methods and techniques; the evaluation of field tensiometer measurements; the automation of the water supply; etc.;

— in drainage design: for the judgement of drainage requirements; the determination of drainage criteria (type of drainage, depth, slope, size and spacing of drains, etc.);

— for the calculation of further hydrophysical parameters (infiltration rate, IR; saturated conductivity, K; unsaturated conductivity, k; etc.) and their evaluation and interpretation.

Various methods can be used for the determination of soil moisture retention curves in the whole suction range. These methods are reviewed by VÁRALLYAY [1973a]. He designed two apparatuses for the determination of soil moisture retention in the low suction range (0—1 atmosphere). Both of them are very suitable for serial analyses. The sand box apparatus (Fig. 4.4) can be used in the suction range pF 0 to 2.0 and the kaolin box apparatus (Fig. 4.5) in the suction range pF 2.0—2.7.

The advantages of the author's apparatus in comparison to similar ones designed in other countries [BAVER, GARDNER and GARDNER 1972; GLOBUS 1969; HARST and STAKMAN 1965] are as follows: filling up the apparatus with the porous medium, i.e. the preparations for the determinations, are much simpler and quicker; the air bubbles are visible and are thus easily detectable in the transparent plexi glass box vacuum chamber and they can be removed simply, during operation, without disturbing the apparatus. Consequently, the apparatus can be used more comfortably, can be controlled more easily and the operational safety is better [VÁRALLYAY 1973a].

In the over-atmosphere suction range the water retention was determined using a pressure-membrane apparatus [STAKMAN and HARST 1969].

In Figure 4.6 water retention curves are presented from our data-collection for some representative soils varying widely in texture, structure, compactness, pH, salinity-alkalinity status and other soil properties.

The soils studied were as follows:

No. 146 Meadow chernozem A-horizon, slightly calcareous loam (Hungarian Danube Valley)

No. 198 Meadow chernozem B-horizon, highly calcareous silty loam (Hungarian Danube Valley)

No. 191 Sandy loess C-horizon (Hungarian Danube Valley)

No. 301 Calcareous Danube alluvium, coarse sand
No. 169 Pseudomyceliar chernozem A-horizon, calcareous loam (Transdanubian Loess Plateau, Érd, Hungary)
No. 349 Meadow chernozem A-horizon, slightly calcareous clay loam (Transtisza Loess Plateau, Törökszentmiklós, Hungary)
No. 140 Meadow soil B-horizon, non-calcareous, heavy-textured sticky clay (Hungarian Tisza Valley, Kisújszállás)
No. 81 Shallow meadow solonetz B-horizon, non-calcareous swelling clay (Hortobágy salt affected area, Transtisza region, Püspökladány, Hungary).

The main properties of these soils are summarized in Table 4.1. The data of moisture retention curves are given in Table 4.2.

The soils are tabulated according to their increasing clay content (water retention).

For the mathematical description of the measured moisture content (θ, in volume %) — suction (matrix potential, ψ, in water column centimetres) relations (i.e. pF-curves) four procedures were applied by the authors [VÁRALLYAY, RAJKAI, PACHEPSKY and MIRONENKO 1979].

The first method was the approximation of the θ-ψ function by fitting a third-degree polynomial equation using multiple regression analysis:

$$y = b_0 + b_1 x + b_2 x^2 + b_3 x^3 \tag{4.5}$$

For fitting the polynom the modified DOOLITTLE procedure was applied and a table-computer programme was developed. It gives and prints the partial regression coefficients (b_0, b_1, b_2 and b_3), data of the analysis of variance (AOV)

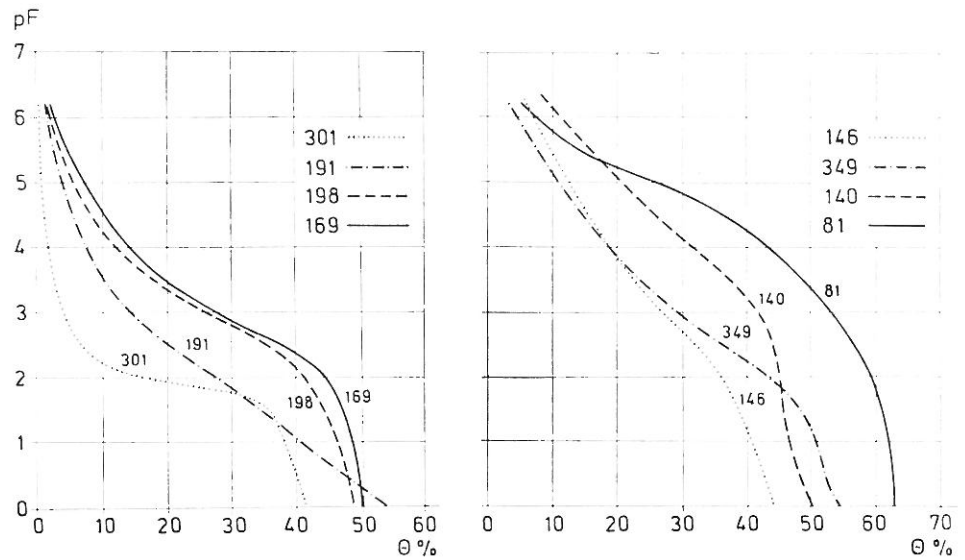

Fig. 4.6
Water retention curves of the studied soils

Table 4.1

Main properties and particle-size distribution of the studied soils

Properties	Soil (Code No)							
	301	191	198	169	146	349	140	81
pH	8.1	8.1	8.2	7.7	8.0	6.9	6.6	8.3
$CaCO_3$-contents, %	25.5	30.1	30.5	7.1	1.2	1.2	—	—
EC mmhos/cm	0.2	0.9	2.2	1.7	0.9	1.7	0.2	1.6
CEC me/100 g soil	6.0	16.3	16.1	24.5	21.2	30.2	31.5	28.5
ESP	1.7	0.2	0.6	0.1	0.5	0.2	2.8	49.4
Organic matter content, %	0.4	0.4	1.9	4.1	2.3	3.1	3.6	1.53
Bulk density g/cm³	1.47	1.27	1.33	1.29	1.51	1.16	1.52	1.27
Particle-size distribution:								
Loss in HCl-treatment	23.53	33.43	33.17	7.38	3.18	3.06	2.03	2.34
1.00—0.25 mm	14.62	4.46	—	4.04	1.99	0.07	0.19	0.55
0.25—0.05 mm	58.77	22.86	11.80	10.68	23.81	8.11	2.82	3.43
0.05—0.01 mm	1.14	24.56	31.81	46.16	31.32	26.67	22.55	32.30
0.01—0.005 mm	0.35	2.48	5.04	5.40	5.27	9.60	8.34	9.02
0.005—0.001 mm	0.15	2.36	6.40	2.83	5.52	14.23	15.56	11.71
<0.001 mm	1.44	9.85	11.78	23.51	28.91	38.26	48.51	40.65
Saturated hydraulic conductivity, cm/day	98.4	32.0	1.8	8.9	1.1	2.0	0.08	0.029

table (SQ, FG and MQ values), the values of the partial and integral F-tests, and the correlation coefficients, R^2.

The points of water-retention curves computed by equation (4.5) are given in Table 4.2. The partial regression coefficients and R values are summarized in Table 4.3. Our experimental results (based on about 500 soil samples, varying widely in such properties as texture, structure, compactness, bulk density, pH, ESP, etc.) proved that this curve-fitting procedure can be successfully applied as a first approximation for the description of water retention curves. The same conclusion can be drawn from the data presented: there are no significant differences between the measured and computed data (Table 4.2) and the high R values (> 0.988) indicate close correlation (Table 4.3). In spite of these facts it can be seen from Table 4.3 that the third members of the polynom (b_3-values) are highly significant, consequently better curve-fitting can be approached by fifth-degree polynoms:

$$y = b_0 + b_1x + b_2x^2 + b_3x^3 + b_4x^4 + b_5x^5 \qquad (4.6)$$

With the application of fifth-degree polynoms there are only negligible differences between the measured and computed data (Table 4.2) and the extremely high correlation coefficients ($R > 0.995$) prove the good practical applicability of this procedure, even for the registration of small differences or minor changes in the water retention curves of various soils (Table 4.3).

The calculation programme was combined with plotter instruction, so the best fitting water-retention curves were drawn automatically. The measured data entered (input) and the calculated values from the AOV table, the partial

Table 4.2

Measured and calculated soil moisture retention data for the studied soils

Soil Code and No. of equations	pF									
	0	0.4	1.0	1.5	2.0	2.3	2.7	3.4	4.2	6.2
301										
Measured	42.3	40.9	38.3	35.9	15.1	8.9	5.4	2.9	2.2	0.3
(4.7)	41.7	41.5	39.8	33.2	17.5	8.7	2.7	0.3	0.0	0.0
(4.14b)	41.4	41.3	40.1	33.1	17.8	8.9	2.2	0.1	0.0	0.0
(4.5)	42.5	41.1	38.4	35.0	11.8	9.0	6.6	3.6	0.6	0.0
(4.6)	42.1	41.1	38.9	33.9	14.4	7.9	5.6	3.4	1.8	0.0
191										
Measured	54.9	48.9	40.8	35.0	28.4	23.5	17.3	10.8	6.9	1.4
(4.7)	54.2	49.7	41.7	34.4	27.2	23.2	18.3	11.5	6.4	1.3
(4.14b)	54.5	49.5	41.4	34.3	27.3	23.4	18.6	11.6	6.0	0.7
(4.5)	53.7	50.8	44.7	34.8	24.1	20.3	16.7	12.1	8.2	1.4
(4.6)	55.0	48.8	41.1	35.0	28.4	23.7	17.5	10.8	6.9	1.4
198										
Measured	54.5	48.6	46.0	44.0	42.1	39.9	33.6	21.4	11.1	1.8
(4.7)	51.2	50.4	48.5	45.7	41.4	38.1	32.7	22.2	11.7	1.4
(4.14b)	51.7	50.9	48.8	45.6	41.1	37.6	32.4	22.4	12.1	0.9
(4.5)	53.0	51.1	47.9	44.5	40.1	36.7	30.9	20.3	12.7	2.2
(4.6)	55.6	49.7	46.3	43.7	41.0	39.0	36.1	19.5	10.8	2.2
169										
Measured	51.6	49.9	48.5	47.7	45.2	41.5	33.2	21.6	12.5	2.7
(4.7)	51.3	50.8	49.4	47.2	43.5	40.2	34.7	23.0	11.2	1.0
(4.14b)	51.0	50.7	49.6	47.4	43.5	40.2	34.7	23.2	11.2	0.4
(4.5)	52.0	50.2	47.9	45.7	42.9	40.7	36.7	20.5	11.6	2.6
(4.6)	51.0	50.2	48.4	46.5	43.8	41.2	33.6	20.7	13.0	2.5
146										
Measured	44.8	43.0	41.5	39.0	36.5	34.0	30.2	23.2	17.1	5.7
(4.7)	44.7	43.6	41.4	38.9	35.8	33.6	30.4	24.1	17.0	5.1
(4.14b)	44.8	43.7	41.4	38.8	35.7	33.5	30.3	24.3	17.4	4.8
(4.5)	45.1	43.5	40.9	38.4	35.6	33.6	30.7	24.8	17.5	4.2
(4.6)	44.6	43.4	41.3	39.0	36.2	34.0	30.4	23.3	17.0	5.7
349										
Measured	54.8	52.8	51.0	48.6	43.6	36.8	33.5	25.0	17.7	4.6
(4.7)	55.3	53.7	50.4	46.7	42.0	38.8	34.2	25.7	16.8	4.2
(4.14b)	55.3	53.7	50.4	46.6	41.9	38.7	34.2	26.0	17.1	3.4
(4.5)	55.6	53.6	50.1	46.6	42.4	39.4	34.8	25.6	16.9	3.9
(4.6)	54.6	53.3	50.9	48.0	43.3	38.8	32.5	24.6	18.0	4.5
140										
Measured	50.2	49.1	46.2	45.4	45.1	44.7	43.5	37.6	28.3	9.3
(4.7)	48.9	48.5	47.8	46.9	45.4	44.2	42.2	37.2	29.1	9.0
(4.14b)	48.7	48.5	47.9	47.0	45.5	44.3	42.2	37.0	29.2	9.2
(4.5)	50.5	49.4	47.7	46.0	44.3	43.1	41.4	37.8	32.2	6.8
(4.6)	49.9	49.1	47.7	46.3	44.7	43.6	41.8	37.7	29.8	9.0
81										
Measured	63.5	63.1	62.7	62.2	61.0	59.4	56.6	50.7	42.5	6.9
(4.7)	62.9	62.7	62.4	61.8	60.8	59.9	58.0	52.2	40.4	8.3
(4.14b)	62.6	62.6	62.4	62.0	61.1	50.1	58.1	51.8	40.1	8.4
(4.5)	65.8	64.5	62.5	60.6	58.5	57.2	55.1	50.9	43.9	6.4
(4.6)	64.3	63.5	62.3	61.0	59.6	58.5	56.8	52.0	40.3	5.5

Table 4.3

The experimentally determined pF-curve parameters

Equation and parameters	Soil (Code No)							
	301	191	198	169	146	349	140	81
(4.7)								
θ_0	41.73	70.02	52.49	52.04	48.01	59.84	49.55	63.06
ψ_0	80.00	29.00	1352.60	1679.00	2581.50	1122.70	38295.20	46769.40
m	1.4594	0.3647	0.5077	0.5746	0.3307	0.3556	0.4030	0.5368
(4.14b)								
θ_0	41.37	74.14	52.48	51.21	47.20	58.65	48.76	62.62
pF_0	1.9125	1.3024	3.1333	3.2564	3.4776	3.1157	4.6324	4.6890
c	1.4415	0.5406	0.4872	0.5824	0.3311	0.3589	0.4005	0.5181
(4.5)								
b_0	4.65	6.73	6.81	7.08	7.16	7.12	7.17	7.09
b_1	$-4.05 \cdot 10^{-1}$	$-3.84 \cdot 10^{-1}$	$-2.94 \cdot 10^{-1}$	$-3.75 \cdot 10^{-1}$	$-2.54 \cdot 10^{-1}$	$-2.56 \cdot 10^{-1}$	$-1.79 \cdot 10^{-1}$	$-1.70 \cdot 10^{-1}$
b_2	$1.96 \cdot 10^{-2}$	$1.02 \cdot 10^{-2}$	$8.13 \cdot 10^{-3}$	$1.29 \cdot 10^{-2}$	$6.62 \cdot 10^{-3}$	$6.06 \cdot 10^{-3}$	$6.16 \cdot 10^{-3}$	$5.22 \cdot 10^{-3}$
b_3	$-3.74 \cdot 10^{-4}$	$-1.01 \cdot 10^{-4}$	$-9.45 \cdot 10^{-5}$	$-1.59 \cdot 10^{-4}$	$-9.99 \cdot 10^{-5}$	$-6.75 \cdot 10^{-5}$	$-1.07 \cdot 10^{-4}$	$-6.50 \cdot 10^{-5}$
(4.6)								
b_0	5.55	6.99	6.90	7.03	7.00	7.01	6.96	7.04
b_1	$-8.81 \cdot 10^{-1}$	$-5.93 \cdot 10^{-1}$	$-3.17 \cdot 10^{-1}$	$-3.71 \cdot 10^{-1}$	$-8.09 \cdot 10^{-2}$	$-1.93 \cdot 10^{-1}$	$-5.32 \cdot 10^{-2}$	$-2.36 \cdot 10^{-1}$
b_2	$8.68 \cdot 10^{-2}$	$3.33 \cdot 10^{-2}$	$2.43 \cdot 10^{-2}$	$1.87 \cdot 10^{-2}$	$1.39 \cdot 10^{-2}$	$4.01 \cdot 10^{-3}$	$4.75 \cdot 10^{-3}$	$1.93 \cdot 10^{-2}$
b_3	$-4.18 \cdot 10^{-3}$	$-9.84 \cdot 10^{-4}$	$5.30 \cdot 10^{-4}$	$-7.16 \cdot 10^{-4}$	$7.37 \cdot 10^{-4}$	$-2.01 \cdot 10^{-4}$	$1.43 \cdot 10^{-4}$	$8.23 \cdot 10^{-4}$
b_4	$9.55 \cdot 10^{-5}$	$1.36 \cdot 10^{-5}$	$-1.80 \cdot 10^{-5}$	$1.60 \cdot 10^{-5}$	$-1.34 \cdot 10^{-5}$	$6.21 \cdot 10^{-6}$	$1.01 \cdot 10^{-7}$	$1.53 \cdot 10^{-5}$
b_5	$-8.45 \cdot 10^{-7}$	$-7.06 \cdot 10^{-8}$	$1.58 \cdot 10^{-7}$	$-1.45 \cdot 10^{-7}$	$6.69 \cdot 10^{-8}$	$-6.39 \cdot 10^{-8}$	$-3.51 \cdot 10^{-8}$	$-1.03 \cdot 10^{-7}$
R								
(4.7)	0.9956	0.9991	0.9946	0.9975	0.9992	0.9974	0.9958	0.9986
(4.14b)	0.9946	0.9990	0.9937	0.9972	0.9986	0.9970	0.9948	0.9984
(4.5)	0.9887	0.9949	0.9931	0.9933	0.9978	0.9974	0.9929	0.9894
(4.6)	0.9950	0.9999	0.9982	0.9974	0.9997	0.9994	0.9954	0.9946

Table 4.4

The influence of various Na-solutions on water retention of soils (Data of pF-curves; moisture content in volume percentage)

Soil Code No	Treatment	pF										ESP
		0	0.4	1.0	1.5	2.0	2.3	2.7	3.4	4.2	6.2	
349	H_2O	54.8	52.8	51.0	48.6	43.6	36.8	33.5	25.0	17.7	4.6	0.2
	NaCl											
350	0.05 N	54.8	53.3	51.3	49.4	43.8	39.6	33.6	26.3	18.1	4.6	4.2
351	0.1 N	51.1	53.6	51.6	50.1	44.5	40.1	35.3	27.6	19.1	4.6	5.9
352	0.5 N	57.4	55.7	53.2	51.3	47.7	44.3	39.3	30.3	20.6	4.6	28.4
	Na_2CO_3											
353	0.05 N	57.5	55.2	53.5	51.2	46.3	42.0	36.6	28.8	20.0	4.6	8.3
354	0.1 N	57.5	56.3	53.9	52.6	48.1	44.2	39.3	30.5	21.7	4.6	30.0
355	0.5 N	59.4	57.3	55.1	54.1	53.5	52.4	49.9	39.8	28.6	4.6	68.2
169	H_2O	51.6	49.9	48.5	47.7	45.2	41.5	33.2	21.6	12.5	2.7	0.1
	NaCl											
170	0.05 N	51.4	50.1	48.9	47.9	45.2	41.7	33.4	21.9	12.6	2.7	3.8
171	0.1 N	52.0	51.2	48.9	47.9	45.3	41.8	34.0	21.9	13.0	2.7	5.1
172	0.5 N	53.6	51.4	49.5	48.3	45.6	11.2	34.1	22.2	14.1	2.7	26.8
	Na_2CO_3											
173	0.05 N	53.0	51.3	51.1	49.5	47.1	43.6	36.4	24.2	14.1	2.6	8.6
174	0.1N	53.4	51.8	51.5	50.7	47.8	45.7	38.6	26.7	17.2	2.8	32.1
175	0.5 N	55.6	54.4	53.6	52.5	51.0	49.5	46.1	32.2	20.6	3.1	61.1

regression coefficients (b_0, b_1, b_2, b_3, b_4, b_5) and the correlation coefficients (R^2) are also indicated as an output of the programme.

Using supplementary programmes any x (moisture content in volume percentage) or y (pF value) point, belonging to a given y or x value, can easily be determined (for instance, soil moisture parameters, etc.).

Another possibility for the approximation of the relationship is the application of the formula:

$$\theta = \frac{\theta_0}{1 + \left(\frac{\psi}{\psi_0}\right)^m} \tag{4.7}$$

where θ_0 = moisture content in volume ratio at full saturation ($\psi = 0$; $\approx$ total porosity)
θ = moisture content in volume ratio at given suction
ψ = suction (water column cm)
ψ_0 and m = experimentally determined constants.

When equation (4.7) is applied, the derivative

$$\frac{\partial \psi}{\partial \theta} = -\frac{\psi_0}{m\theta_0} \cdot \frac{\left[1 + \left(\frac{\psi}{\psi_0}\right)^m\right]^2}{\left(\frac{\psi}{\psi_0}\right)^{m-1}} \tag{4.8}$$

Table

Measured and calculated soil moisture retention data

Soil (Code and No. of equations	pF									
	0	0.4	1.0	1.5	2.0	2.3	2.7	3.4	4.2	6.2
349										
Measured	54.8	52.8	51.0	48.6	43.6	36.8	33.5	25.0	17.7	4.6
(4.7)	55.3	53.7	50.4	46.7	42.0	38.8	34.2	25.7	16.8	4.2
(4.14b)	55.3	53.7	50.4	46.6	41.9	38.7	34.2	26.0	17.1	3.4
(4.5)	55.6	53.6	50.1	46.6	42.4	39.4	34.8	25.6	16.9	3.9
(4.6)	54.6	53.3	50.9	48.0	43.3	38.8	32.5	24.6	18.0	4.5
352										
Measured	57.4	55.7	53.2	51.3	47.7	44.3	39.3	30.3	20.6	4.6
(4.7)	57.1	56.0	53.8	50.9	47.1	44.2	39.7	30.7	20.3	4.6
(4.14b)	57.1	56.1	53.8	50.9	46.9	44.0	39.6	30.8	20.7	4.0
(4.5)	57.8	56.0	53.1	50.3	46.9	44.5	40.7	31.7	19.9	4.1
(4.6)	57.3	55.8	53.4	50.7	47.2	44.3	39.5	29.7	20.6	4.6
353										
Measured	57.5	55.2	53.5	51.2	46.3	42.0	36.6	28.8	20.0	4.6
(4.7)	57.5	56.1	53.3	49.9	45.5	42.4	37.8	28.9	19.2	4.8
(4.14b)	57.5	56.2	53.3	49.8	45.4	42.3	37.8	29.2	19.6	4.1
(4.5)	57.8	55.9	52.5	49.1	45.2	42.4	38.2	29.2	19.5	4.2
(4.6)	57.3	55.8	53.0	50.0	45.7	42.3	37.1	28.3	20.1	4.5
354										
Measured	57.5	56.3	53.9	52.6	48.1	44.2	39.3	30.5	21.7	4.6
(4.7)	57.7	56.6	54.2	51.3	47.4	44.5	40.0	31.1	20.7	4.9
(4.14b)	57.7	56.7	54.3	51.3	47.3	44.4	40.0	31.3	21.2	4.3
(4.5)	58.3	56.6	53.6	50.7	47.3	44.9	41.0	32.0	20.3	4.2
(4.6)	57.5	56.4	54.3	51.9	48.4	45.1	39.2	30.1	22.1	4.5
355										
Measured	59.4	57.3	55.1	54.1	53.5	52.4	49.9	39.8	28.6	4.6
(4.7)	57.6	53·7	56.5	55.4	53.5	51.8	48.8	40.7	28.1	5.0
(4.14b)	57.4	57.2	56.7	55.6	53.7	51.9	48.6	40.5	28.5	4.8
(4.5)	59.2	58.1	56.2	54.4	52.3	50.9	48.8	43.7	47.1	3.8
(4.6)	58.9	58.0	56.3	54.7	52.7	51.3	49.0	42.7	27.5	4.8

becomes infinity if: $\psi = 0$, $m > 1$; and it is zero if: $\psi = 0$, $m < 1$. This is in good agreement with the statement by BEAR, ZASLAVSKY and IRMAY [1968] (where $\eta = -\psi$, $c = \theta$): "In some well aggregated soils the derivative $\frac{\partial \eta}{\partial c}$ is very low, and in other cases it is very high." The above mentioned derivative in our experiment proved to be neither zero nor infinity. Consequently, equation (4.8) cannot be used directly for the approximation of the θ-ψ relationship. Therefore equation (4.8) was slightly modified, introducing small ε_ψ values in addition to ψ:

$$\theta = \frac{\theta_0 \left[1 + \left(\frac{\varepsilon_\psi + \psi}{\psi_0} \right)^m \right]}{1 + \left(\frac{\psi + \varepsilon_\psi}{\psi_0} \right)^m} \tag{4.9}$$

5.4

and pF curve parameters for soils saturated with Na^+ to various degree

No. of equations and parameters	Soil (Code No)				
	349	352	353	354	355
(4.7)					
θ_0	59.84	59.55	61.09	60.34	58.07
ψ_0	1 122.70	2 932.30	1 880.60	2 931.60	13 927.10
m	0.3556	0.3926	0.3659	0.3844	0.4991
(4.14b)					
θ_0	58.65	58.56	59.98	59.28	57.51
pF_0	−3.1157	−3.5206	−3.3373	−3.5284	−4.1822
c	0.3589	0.3926	0.3682	0.3858	0.4854
(4.5)					
b_0	7.12	7.08	7.06	7.07	7.13
b_1	$-2.56 \cdot 10^{-1}$	$-2.37 \cdot 10^{-1}$	$-2.23 \cdot 10^{-1}$	$-2.31 \cdot 10^{-1}$	$-2.78 \cdot 10^{-1}$
b_2	$6.06 \cdot 10^{-3}$	$6.05 \cdot 10^{-3}$	$4.97 \cdot 10^{-3}$	$5.75 \cdot 10^{-3}$	$9.31 \cdot 10^{-3}$
b_3	$-6.75 \cdot 10^{-5}$	$-7.04 \cdot 10^{-5}$	$-5.59 \cdot 10^{-5}$	$-6.64 \cdot 10^{-3}$	$-1.12 \cdot 10^{-4}$
(4.6)					
b_0	7.01	7.00	7.00	7.00	6.99
b_1	$-1.93 \cdot 10^{-1}$	$-1.93 \cdot 10^{-1}$	$-1.93 \cdot 10^{-1}$	$-2.18 \cdot 10^{-1}$	$-1.90 \cdot 10^{-1}$
b_2	$4.01 \cdot 10^{-3}$	$4.76 \cdot 10^{-3}$	$4.93 \cdot 10^{-3}$	$1.08 \cdot 10^{-2}$	$5.72 \cdot 10^{-3}$
b_3	$-2.01 \cdot 10^{-4}$	$-1.53 \cdot 10^{-4}$	$-1.78 \cdot 10^{-4}$	$-5.05 \cdot 10^{-4}$	$-1.57 \cdot 10^{-4}$
b_4	$6.21 \cdot 10^{-6}$	$3.54 \cdot 10^{-6}$	$4.11 \cdot 10^{-6}$	$1.12 \cdot 10^{-5}$	$3.30 \cdot 10^{-6}$
b_5	$-6.38 \cdot 10^{-8}$	$-3.39 \cdot 10^{-8}$	$-3.72 \cdot 10^{-8}$	$-8.93 \cdot 10^{-8}$	$-3.28 \cdot 10^{-8}$
R					
(4.7)	0.9974	0.9997	0.9990	0.9992	0.9981
(4.14b)	0.9970	0.9996	0.9989	0.9992	0.9978
(4.5)	0.9974	0.9991	0.9990	0.9978	0.9946
(4.6)	0.9994	0.9998	0.9996	0.9997	0.9959

In the high suction range ($pF \geq 0.5$) this modification is not necessary because ε_ψ is very low in comparison to ψ and there is only a negligible difference between ψ and $\psi + \varepsilon_\psi$. At low suction the proposed modification means that the $\frac{\partial \psi}{\partial \theta}$ derivative will not be zero or infinity:

$$\left.\frac{\partial \psi}{\partial \theta}\right|_{\psi=0} = -\frac{\psi_0}{m\theta_0} \cdot \frac{\left[1 + \left(\frac{\varepsilon_\psi}{\psi_0}\right)^m\right]^2}{\left(\frac{\varepsilon_\psi}{\psi_0}\right)^{m-1}} \tag{4.10}$$

If $0.5 < pF < 5-7$ and $\varepsilon_\psi = 0$ (or can be neglected) m and ψ_0 are determined from the θ-ψ relations (upper part of the pF-curve) using equation (4.8). In the low suction range ($0.5 > pF$) the ε_ψ value can be computed from the θ-ψ relations with equation (4.10).

Based on the measured water retention data given in Tables 4.2 and 4.4, the experimentally determined parameters of equation (4.7), ψ_0 and m,

were calculated (Tables 4.3 and 4.5). The measured and calculated values were compared by applying the least square method:

$$\Delta = \sqrt{\frac{1}{10}\sum_{i=10}^{10}(\theta_i - \bar{\theta}_i)^2} = \min \tag{4.11}$$

or

$$\delta = 100\% \sqrt{\frac{1}{10}\sum_{i=10}^{10}\left(1 - \frac{\bar{\theta}_i}{\theta_i}\right)^2} = \min \tag{4.12}$$

The maximum correlation coefficients between measured and calculated data can be obtained from the following equation:

$$R = \frac{\sum_{i=1}^{10}\theta_i\,\bar{\theta}_i - \frac{1}{10}\sum_{i=1}^{10}\theta_i \sum_{i=1}^{10}\bar{\theta}_i}{\sqrt{\left[\sum_{i=1}^{10}\bar{\theta}_i^2 - \frac{1}{10}\left(\sum_{i=1}^{10}\bar{\theta}_i\right)^2\right]\left[\sum_{i=1}^{10}\theta_i^2 - \frac{1}{10}\left(\sum_{i=1}^{10}\theta_i\right)^2\right]}} = \max \tag{4.13}$$

As is shown in Tables 4.2 and 4.5 there are only small differences between the measured and calculated values and the high correlation coefficients (R values in Tables 4.3 and 4.5) prove that this procedure also represents a good approach for the mathematical description of water retention curves.

The fourth formula proposed for the description of θ-ψ relationships is:

$$\theta = \frac{\theta_0}{2}\,\mathrm{erfc}\,(b + c \cdot \mathrm{pF}) \tag{4.14a}$$

or in another form:

$$\theta = \frac{\theta_0}{2}\,\mathrm{erfc}\,[c(\mathrm{pF} + \mathrm{pF}_0)] \tag{4.14b}$$

where θ = the moisture content at given ψ or pF
θ_0 = the moisture content at full saturation ($\psi = 0$)
b, c or c, pF_0 = experimentally determined parameters
erfc = the error function

$$\mathrm{erfc}\,(z) = \frac{2}{\sqrt{\pi}}\int_z^\infty e^{-t^2}\,\mathrm{d}t \tag{4.15}$$

The c and pF_0 parameters are given in Tables 4.3 and 4.5. The measured and calculated values (Tables 4.2 and 4.5) are in good agreement within the whole suction range for soils varying widely in physical and chemical properties. The good agreement between measured and calculated values is also reflected by the high correlation coefficients (R values in Tables 4.2 and 4.5).

The expression for the derivative of θ with respect to ψ is:

$$\frac{\partial\psi}{\partial\theta} = \frac{b\,\theta_0}{2} \cdot 2.0326\,\frac{1}{\psi}\,e^{-(a+b\lg\psi)^2} \tag{4.16}$$

$$\lim_{\psi \to 0} \left(\frac{\partial \theta}{\partial \psi} = 0 \right).$$

These procedures give a good possibility for the numerical classification of soils according to their hydrophysical characteristics [HILLEL 1971; RIJTEMA 1965; Soil Physical Condition . . . 1975; VÁRALLYAY 1973a, 1976b, 1978a; VÁRALLYAY, RAJKAI, PACHEPSKY and MIRONENKO 1979; Water in Heavy Soils 1976] and represent an exact basis for the mapping of these soil properties and for planning the various actions of agricultural water management. The mathematically described pF-curves provide possibilities for the estimative calculation of other hydrophysical properties (saturated and unsaturated conductivity, etc.), as well.

The characteristics of the pF-curve depend on the shape and size distribution of the soil pores in the heterogeneous soil matrix which is determined by the size, shape and spatial arrangement of the elementary solid particles, the micro- and macro-aggregates and the larger structural units (tortuosity factor, etc.). Consequently, any factor affecting the pore-size distribution of soils (texture, structure and its stability, compactness, Na^+-saturation, dispersion, swelling, etc. and their influencing factors) influences water retention and determines the pF curves.

As is shown by the water retention data (Table 4.2) and clearly illustrated by the pF-curves presented (Fig. 4.6), in coarse-textured soils the moisture content sharply decreases with increasing suction, because water can be drained from their large pores by small pulling forces (suction). In medium-textured, and especially in heavy-textured, swelling soils the moisture content decreases only moderately with increasing suction and this decrease is considerable only in the high suction range because the liquid stored in small pores and/or bound on the large specific surface of clay particles and soil colloids (various sorption forces), sometimes interstratified between the lattice layers of expended clay minerals, can be drained (extracted) only by high driving forces (suction gradient).

The cracks, worm-holes, root-channels and large inter-aggregate pores are already drained in the lowest suction range (pF 0 – 0.4). The heterogeneous pore-size distribution (monotonous slope in the pF curves) generally indicated the favourable structural status of the soil (water and air may be present simultaneously). In the high suction range pF-curves are determined by the micropore size distribution, influenced mostly by the micro aggregate-status and texture.

Two simplified and generalized conclusions can be drawn in this respect:

a) Water retention increases with increasing clay and colloid content (heavier texture) within the whole suction range.

b) With increasing density (compactness) the volume of the large pores (especially gravitational pore-space) decreases, but water retention increases in the high suction range. Consequently, the available moisture range decreases, sometimes to a great extent [BAVER, GARDNER and GARDNER 1972; HILLEL 1971; International Source Book 1967; KUTILEK 1973; MICHURIN 1975; RODE 1965; ROSE 1966; VÁRALLYAY 1973a, 1978c; Water in Heavy Soils 1976].

The influence of salinity-alkalinity on the matric potential (ψ) is a much more complicated phenomena and it is directly or indirectly related to changes

in the physical status of the soil due to the relationships between the solid and liquid phases of the soil.

The alkalization (high Na^+-saturation) of soils, especially of heavy-textured soils with a high swelling clay content causes increased hydration, swelling, dispersion of soil colloids, aggregate and structure destruction and clogging of macropores, i.e. significant, sometimes radical changes in the pore size distribution: the pore size and macropore volume decreases while the micropore volume increases [KIRKHAM and POWERS 1972; MCNEAL et al. 1968; VÁRALLYAY 1972, 1977, 1974c]. These changes are clearly reflected by the water retention curves.

In Table 4.4 the data of a laboratory model-experiment are summarized. The influence of various Na-solutions (0.05N, 0.1N and 0.5N NaCl and Na_2CO_3) on the water retention of Törökszentmiklós clay loam (No. 349) and Érd loam (No. 169) was studied [VÁRALLYAY 1976b].

A description of the soils, with their main properties, was given earlier in this chapter (Table 4.1).

The fragmented air-dry soil samples were uniformly packed (volume weights were 1.16 $\pm$ 0.02 g/cm^3 and 1.29 $\pm$0.02 g/cm^3 for No. 349 and No. 169 soils, respectively) into a 100 cm^3 (height 5 cm, surface 20 cm^2) brass cylinder. The soils were saturated with the above mentioned solutions. For the prevention of swelling (volume changes) perforated plastic caps were used to close the upper end of the cylinder. After full saturation pF-curves were determined by the previously described procedure.

Water retention data are given in Table 4.4, the mathematically described pF-curve parameters are shown in Table 4.5 and some of the data are illustrated in Figure 4.7 [VÁRALLYAY 1976b].

The influence of a neutral sodium salt (NaCl) proved to be insignificant in the concentration range studied (low Na^+-saturation). The effect of 0.5N NaCl results in a moderate swelling (the lower ends of the samples are covered only by a nylon cloth) (pF 0) and a slight increase in the wilting percentage (pF 4.2).

Under the effect of a sodium salt capable of alkaline hydrolysis (Na_2CO_3), as the concentration increased (increasing ESP) the water retention also increased within the whole suction range, thus resulting in higher "total porosity" ($\psi = 0$), "field capacity" (pF 2.3 – 2.7) and "wilting percentage" (pF 4.2). In the contrary case, due to the large pores → fine pores pore-size redistribution (aggregate destruction, dispersion, peptization, hydration, swelling, etc.) the gravitational pore-space decreased (Table 4.4, Fig. 4.7). Consequently, in such cases the effectivity and efficiency of normal drainage methods are rather limited [DI GLÉRIA, KLIMES-SZMIK and DVORACSEK 1957; HADAS et al. 1973; HILLEL 1972; International Source Book 1967; KOVÁCS 1976; Proc. Symp. ISSS Subcomm. 1965, 1969, 1975; Salinity Problems . . . 1961; SZABOLCS 1971b, 1974; VÁRALLYAY 1977, 1978a, 1978b; Water in Heavy Soils 1976]. These changes are expressed more clearly in the Törökszentmiklós clay loam than in the Érd loam.

The available moisture range (AMR), calculated as the difference between the "field capacity" (pF 2.0–2.7) and the "wilting percentage" (pF 4.2) increased parallel with the ESP, which is quite contrary to the classical explanation of the inadequate water supply of plants in alkali soils and which proved the opinion of KUTILEK [1973], VÁRALLYAY [1976a, 1977] and others [ARYA

1973; DIESTEL 1974; HADAS et al. 1973; KIRKHAM and POWERS 1972; NIELSEN 1972; OLSZTA 1975; RIJTEMA 1968; RUSSEL 1973] that in such cases it is not the low AMR which is the main limiting factor of availability of soil moisture, but the very low flux of water to the roots through the relatively dry moisture depletion zone, in which the transport coefficients (k and D) are extremely low. This phenomenon is clearly illustrated by the results of an

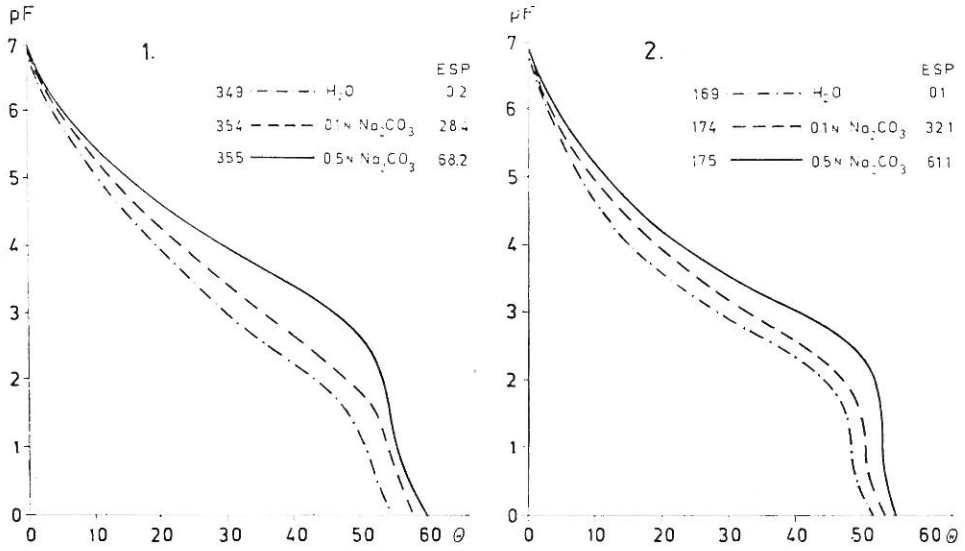

Fig. 4.7
Water retention curves of a clay loam (1) and a loam (2) saturated with Na_2CO_3 solutions of various concentrations

evaporation-column model experiment [VÁRALLYAY 1976a]. As can be seen from the moisture-profile redistribution curves (Fig. 4.18), the drying was practically uniform within the whole columns in the case of water and diluted NaCl solutions, but in the Na_2CO_3-treated (sodium saturated) variants the evaporated water could not be replaced from the relatively moist deeper layers in spite of the high suction gradient, because of the very low transport coefficients. The establishment of a permanent vegetation with a dense root system has significant importance under such ecological conditions, especially from the viewpoint of the rational use of the limited moisture resources of soils.

4.2. Salinity-alkalinity and liquid flow in the saturated zone

The saturated flow is of considerable importance in many aspects of agricultural and urban life:

— in hydrological and hydrogeological research (for the determination of feeding, horizontal and vertical movement of various subsurface waters, for seepage flow analysis, etc.),

— in ground water hydrology (for the determination, description and prediction of the ground water regime, the depth to the water table, the

fluctuation in the ground water level, and the evaluation of factors influencing the ground water regime, etc.);

— in drainage design and practice for agricultural and engineering purposes (for the selection of the optimum drainage combination, type of drainage, depth, slope, size of drains, drain spacing, etc.) [International Source Book 1967; Salinity Problems . . . 1961; VÁRALLYAY 1972; Water in Heavy Soils 1976; WORTHINGTON 1977].

In the soil, except for the layers below the water table, saturated conditions are not frequent (permanently or temporarily flooded areas, layers with stagnant water within the soil profile above an impermeable horizon, etc.), and so the saturated flow data can be interpreted directly only for such conditions. But these data can be used as a sensitive and well-defined indicator for the characterization of the physical and water properties of soils (porosity, pore-size distribution, aggregate stability, permeability, etc.) for the registration of changes in the above-mentioned properties due to natural factors or human activities (agrotechnics, tillage, amelioration, irrigation, etc.) and can serve as a good basis for the determination of further parameters (capillary flow, etc.) [BAVER, GARDNER and GARDNER 1972; CHILDS 1969; GLOBUS 1969; HILLEL 1971, 1972; International Source Book 1967; KOVÁCS 1976; RODE 1965; Soil Physical Conditions 1975; VÁRALLYAY 1972].

Saturated flow, as each flux in general, is a function of the gradient of the driving force and conductivity and may be expressed as:

$$V = -K \cdot \operatorname{grad} H \tag{4.17}$$

where V = velocity of saturated flow (cm/day)
K = saturated hydraulic conductivity (cm/day)
$\operatorname{grad} H$ = hydraulic gradient.

It is well known that the geometry of soil pores and pore-size distribution rather than total pore volume govern hydraulic conductivity.

In saturated soil layers all of the pores are filled with water, consequently, as a first approximation (assuming that the solid phase, porosity and pore-size distribution are constant) the saturated hydraulic conductivity can be characterized by a single value (K = cm/day). Under natural conditions this is true only for soils of good structure and aggregate stability, for structureless coarse sands, etc. In other cases, during the filtration of the soil solution a mechanical compaction or solid-liquid phase interactions take place and the hydraulic conductivity changes, sometimes to a great extent. These changes are particularly significant in layered, salt affected soils, where the soil is far from being an ideal two or three phase system, the moving fluid is a salt solution of different concentration and ion-composition and where reversible and/or irreversible interactions exist between the solid and liquid phases. For the study of saturated flow phenomena various model experiments were carried out [VÁRALLYAY 1972, 1973b, 1974c, 1978b; VÁRALLYAY and SZABOLCS 1974, 1978].

In the first experiment the hydraulic conductivity of various Hungarian salt affected soils were determined and the relationships between the K-values, their change with time and soil properties were studied.

Soil samples were taken from the various genetic horizons and layers of 3 representative soil profiles:

M-11 Sodic solonchak on calcareous Danube alluvium (Danube Valley, Hungary)
M-14 Shallow meadow solonetz on calcareous loess-like clay (Tisza Valley, Hortobágy, Hungary)
M-16 Meadow soil solonetzic in deeper layers, on calcareous loess-like clay (Tisza Valley, Hortobágy, Hungary).

The soils were characterized by detailed laboratory analyses (Tables 4.6 and 4.7). Illite was the dominant clay mineral in the fine fraction of the soils studied, but in the Hortobágy soils (M-14, M-16) the montmorillonite content was also significant.

The saturated hydraulic conductivity was determined on fragmented soil samples in the laboratory with constant ($K > 15$ cm/day) or falling head ($K < 15$cm/day) method using distilled water. Two apparatuses were constructed for serial analyses of the saturated hydraulic conductivity [VÁRALLYAY 1972].

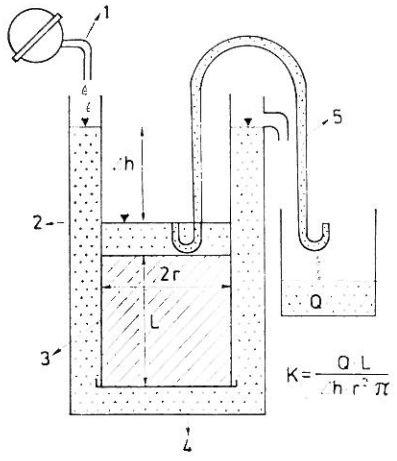

Fig. 4.8
Constant head apparatus for the laboratory determination of hydraulic conductivity. 1. Tap. 2. Constant level measuring tank with overflow. 3. Brass cylinder and fitting tube with rubber 0-ring seal. 4. Nylon cloth. 5. Siphon. 6. Soil sample

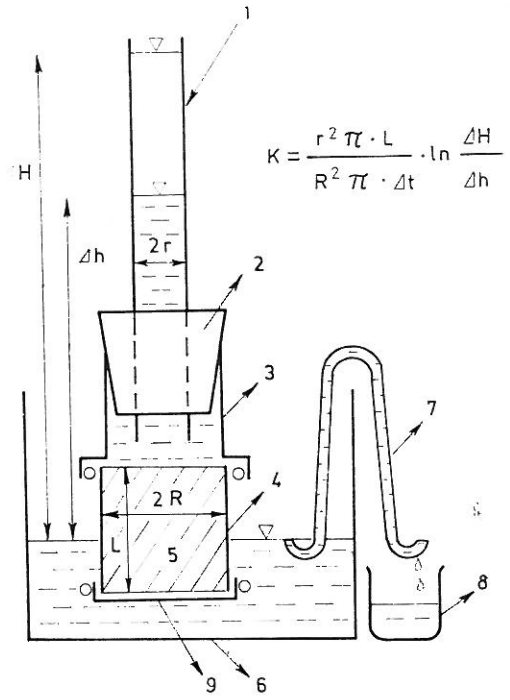

Fig. 4.9
Falling head apparatus for the laboratory determination of hydraulic conductivity. 1. Glass tube. 2. Rubber stopper. 3. Fitting tube with rubber 0-ring seal. 4. Brass cylinder. 5. Soil sample. 6. Constant level measuring tank. 7. Siphon. 8. Glass beaker. 9. Nylon cloth

The constant-head and falling-head apparatuses are shown in Figures 4.8 and 4.9, respectively. Saturated conductivity values were computed with the DARCY formula, using equations (4.18) and (4.19):

$$K = \frac{Q \cdot L}{\Delta h_c \cdot r^2 \pi} \qquad (4.18)$$

Table 4.6

Some main characteristics of salt affected soils studied in the hydraulic conductivity model experiment

Profile No and genetic horizon	Sampling depth cm	pH		$CaCO_3$ %	Bulk density g/cm³		Total salt content, %		Organic matter
		i	ii		i	ii	i	ii	
M-11									
1	0—4	9.1	9.2	9.6	1.36	0.98	1.20	0.01	1.25
2	4—16	9.0	9.2	13.3	1.33	1.09	0.45	0.06	0.79
3	16—29	8.9	9.1	20.1	1.31	1.07	0.17	0.09	0.60
4	29—41	8.8	9.0	35.4	1.28	1.10	0.18	0.00	
	41—55	8.6	8.8	32.0	1.31	1.21	0.24	0.00	
5	55—70	8.2	8.3	22.2	1.37	1.30	0.13	0.00	
	70—90	8.3	8.6	20.6	1.37	1.30	0.11	0.00	
6	90—110	8.2	8.5	28.2	1.32	1.28	0.17	0.00	
	110—125	8.3	8.3	15.1	1.49	1.40	0.08	0.00	
M-14									
A	0—3	5.6	6.2	—	0.73	0.98	0.06	0.02	5.87
B_1	3—15	7.9	8.0	—	1.27	1.05	0.27	0.18	2.22
B_2	15—25	8.3	8.2	—	1.27	0.92	0.51	0.18	1.53
	25—38	8.7	8.9	—	1.27	0.89	0.75	0.30	1.52
	38—55	9.0	9.1	2.5	1.30	0.98	0.75	0.23	1.14
BC	55—66	8.7	9.3	14.3	1.24	0.97	0.74	0.16	
	66—79	9.1	9.1	17.7	1.23	1.01	0.47	0.17	
C	79—100	9.1	9.3	14.0	1.23	0.98	0.38	0.16	
	100—125	9.1	9.4	13.0	1.23	0.98	0.29	0.14	
M-16									
A	0—10	6.7	7.3	—	1.10	1.02	0.03	0.02	2.30
	10—20	6.8	7.5	—	1.13	1.05	0.03	0.02	1.64
B_1	20—35	8.2	8.1	2.5	1.23	1.08	0.10	0.05	1.76
	35—50	8.4	8.5	5.1	1.29	1.20	0.14	0.05	1.31
B_2	50—65	8.7	8.8	13.4	1.26	1.20	0.07	0.04	0.57
C_1	65—80	8.9	9.1	20.0	1.29	1.26	0.09	0.03	
	80—100	8.9	9.3	21.0	1.26	1.24	0.09	0.02	
C_2	100—125	8.9	9.2	20.2	1.29	1.26	0.09	0.01	

i = At the beginning of the experiment
ii = At the end of the experiment

where K = saturated hydraulic conductivity (cm/day)
Q = quantity of water filtrating through the soil column (cm^3/day)
L = length of the soil column (cm)
$r^2\pi$ = surface area of the soil column (cm^2)
Δh_c = constant hydraulic head (cm), difference between the outside and inside constant water level

$$K = \frac{r^2\pi \cdot L}{R^2\pi \cdot \Delta t} \cdot \ln \frac{\Delta H}{\Delta h} \qquad (4.19)$$

Table 4.7

Particle-size distribution and absorption properties of salt affected soils studied in the hydraulic conductivity model experiment

Profile No and genetic horizon	Sampling depth cm	Loss in HCl treatment %	Particle size distribution, %						CEC	ESP
			1.00 – 0.25	0.25 – 0.05	0.05 – 0.01	0.01 – 0.005	0.005 – 0.001	<0.001		
			mm							
M-11										
1	0—4	10.73	12.00	52.36	13.80	2.62	4.52	3.97	11.58	45.80
2	4—16	15.52	9.61	39.58	12.65	3.14	5.57	13.93	16.80	54.61
3	16—29	21.80	6.11	36.18	11.10	2.73	7.63	14.45	12.45	50.11
4	29—41	35.55	6.26	30.69	8.31	3.00	6.62	9.57	9.42	42.03
	41—55	34.00	6.34	40.08	7.52	1.89	3.01	7.16	7.01	49.92
5	55—70	22.71	8.75	58.17	4.15	0.38	2.11	3.73		
	70—90	21.23	11.01	56.97	5.39	0.31	3.22	1.87		
6	90—110	28.33	12.31	42.93	9.29	2.30	3.38	1.46		
	110—125	15.01	44.99	35.34	2.75	0.00	1.11	0.80		
M-14										
A	0—3	1.49	0.83	15.07	48.96	10.08	11.65	11.92	8.99	12.65
B_1	3—15	2.10	1.44	4.08	37.74	9.29	11.54	33.81	22.34	66.15
B_2	15—25	2.34	0.55	3.43	32.30	9.02	11.71	40.65	28.52	49.43
	25—38	2.41	0.15	2.63	31.27	7.85	10.29	45.40	35.53	58.68
	38—55	2.94	0.01	2.14	32.86	9.69	11.12	41.24	24.03	54.93
BC	55—66	15.02	0.01	4.15	29.31	8.44	10.55	32.52		
	66—79	18.36	0.06	4.08	28.83	8.42	9.00	31.25		
C	79—100	16.00	0.05	3.53	32.74	10.61	7.56	29.42		
	100—125	15.39	0.12	2.76	34.85	9.56	11.79	25.53		
M-16										
A	0—10	1.94	0.17	30.16	32.82	4.04	6.90	23.97		
	10—20	2.34	0.04	29.25	31.49	5.74	6.98	24.16		
B_1	20—35	4.59	0.00	24.20	28.42	5.80	7.78	29.21		
	35—50	7.65	0.00	26.65	27.53	4.25	6.48	27.44		
B_2	50—65	15.98	0.00	23.64	27.16	4.62	4.11	24.49		
C_1	65—80	22.99	0.00	20.39	27.06	3.68	6.78	19.10		
	80—100	22.80	0.00	22.61	25.44	4.24	5.29	19.62		
C_2	100—125	20.84	0.00	23.98	25.88	4.51	4.20	20.59		

where K, L = see above
$r^2\pi$ = surface area of the liquid-container tube (cm^2)
$R^2\pi$ = surface area of the column (cm^2)
Δt = time-interval of the measurement (day)
ΔH = hydraulic head (mm) at the beginning of the measurement
Δh = hydraulic head (mm) at the end of the measurement

The K-values and their changes with time were usually measured twice daily until the stabilization, on fragmented soil samples (packed uniformly into a brass cylinder with a height of 5 cm and a volume of 100 cm^3), with distilled water (Table 4.8). The changes in the bulk density, pH and total salt content during the experiment were also determined (Table 4.6). The measurements were made in three replicates and each figure represents the average of these replicates.

Table 4.8

Changes in saturated hydraulic conductivity (K = cm/day) as a function of time in salt affected soils

Observation period t = hours	Sampling depth, cm								
	0 - 4	4 - 16	16 - 29	29 - 41	41 — 55	55 - 70	70 — 90	90—110	110 - 125
Solonchak, Profile M-11									
0—2	2.4	0.30	0.085	0.097	0.46	1.4	3.1	0.96	212
2—5	1.5	0.27	0.053	0.078	0.43	0.75	1.8	0.97	204
5—9	0.70	0.24	0.037	0.070	0.40	0.73	1.7	0.93	201
9—14	0.47	0.23	0.035	0.064	0.25	0.53	1.4	0.72	219
14—26	0.19	0.19	0.031	0.049	0.19	0.50	1.5	0.64	217
26—38	0.14	0.16	0.025	0.041	0.17	0.52	1.5	0.54	
38—43	0.11	0.15	0.020	0.037	0.16	0.50	1.5	0.51	
43—58	0.082	0.12	0.021	0.030	0.12	0.49	1.5	0.50	
58—66	0.069	0.11	0.018	0.030	0.10	0.48	1.9	0.46	
66—74	0.048	0.098	0.020	0.029	0.091	0.53	1.9	0.46	
74—90	0.049	0.093	0.021	0.028	0.081	0.56	1.9	0.43	
90—98	0.041	0.081	0.021	0.028	0.074	0.53	2.2	0.42	
98—114	0.043	0.083	0.022	0.027	0.074	0.52		0.43	
114—122	0.042	0.080	0.019	0.026	0.061	0.52		0.43	
122—138	0.043	0.079	0.019	0.025	0.069	0.55		0.45	
138—146	0.045	0.074	0.018	0.024	0.063	0.57		0.44	
146—162	0.044	0.068	0.019	0.022	0.061	0.60		0.45	
162—170	0.039	0.069	0.018	0.022	0.055	0.58		0.44	
	Sampling depth, cm								
	0—3	3—15	15—25	25—38	38—55	55—66	66—79	79 —100	100—125
Shallow meadow solonetz, Profile M-14									
0—6	27	0.0037	0.29	0.0074	0.0083	0.13	0.041	0.014	0.010
6—30	36	0.0036	0.16	0.0060	0.0088	0.051	0.033	0.013	0.0046
30—54	36	0.0035	0.10	0.0063	0.0090	0.025	0.031	0.011	0.0042
54—78	41	0.0035	0.046	0.0065	0.011	0.019	0.028	0.010	0.0041
78—92	41	0.0035	0.036	0.0060	0.010	0.015	0.026	0.0095	0.0041
92—164	43	0.0034	0.016	0.0061	0.0084	0.010	0.020	0.0078	0.0039
164—188	39	0.0032	0.013	0.0063	0.0073	0.0090	0.016	0.0060	0.0036
188—212	35	0.0030	0.010	0.0056	0.0071	0.0078	0.012	0.0058	0.0036
212—236	38	0.0038	0.010	0.0058	0.0076	0.0080	0.012	0.0064	0.0035
236—260	36	0.0028	0.010	0.0058	0.0070	0.0073	0.012	0.0064	0.0036
260—332	28	0.0031	0.011	0.0059	0.0071	0.0070	0.012	0.0059	0.0035
332—356	28	0.0028	0.0069	0.0051	0.0068	0.0055	0.0076	0.0049	0.0027
356—380	26	0.0026	0.0073	0.0051	0.0061	0.0047	0.0086	0.0048	0.0026
	Sampling depth, cm								
	0 —10	10—20	20—35	35—50	50 —65	65 - 80	80 —100	100 —125	
Meadow soil, solonetzic in deeper layers, Profile M-16									
0—6	39	33	24	24	19	4.7	5.9	5.2	
6—14	38	33	24	24	18	4.4	5.8	5.1	
14—30	31	30	21	23	16	4.0	5.2	4.2	
30—38	31	29	21	22	15	3.5	5.1	4.0	
38—54	32	28	22	23	18	3.8	5.4	3.9	
54—62	32	27	22	22	17	3.7	5.2	3.7	
62—78	35	30	24	24	18	3.7	5.2	3.7	
78—86	33	31	22	23	17	3.6	5.4	3.6	
86—102	33	30	22	24	17	3.9	5.4	3.7	
102—174	32	32	21	23	17	3.7	5.2	3.9	
174—182	33	31	21	22	17	3.7	5.3	3.9	

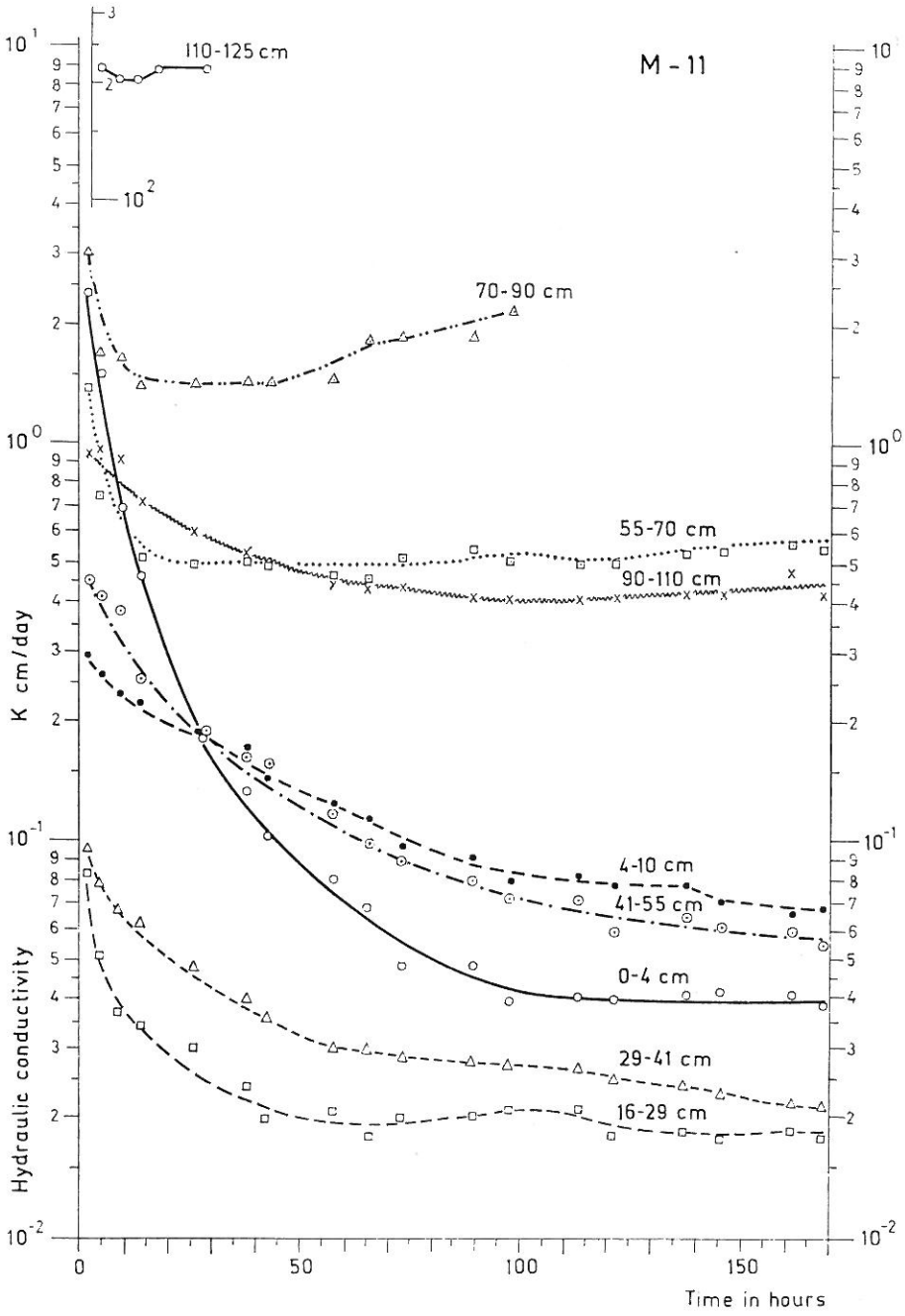

Fig. 4.10
Permeability curves of a solonchak profile (saturated conductivity changes in time)

The hydraulic conductivity data measured (K = cm/day) were plotted against time on a semilogarithmic scale and these permeability curves are given for the M-11, M-14 and M-16 profiles in Figures 4.10, 4.11 and 4.12, respectively.

There were great differences in the hydraulic conductivity of different soil types and various horizons.

The high hydraulic conductivity of the A-horizons was due to the low ESP values, coarser texture and higher organic matter content (mainly root-residues).

It is well known that pore-size distribution [BAVER, GARDNER and GARDNER 1972; CHILDS,1969; KIRKHAM and POWERS 1972; NERPIN and CHUDNOVSKY 1967, 1975] rather than total pore volume affects hydraulic conductivity. The macropore volume and consequently the hydraulic conductivity in salt affected soils were influenced mainly by aggregate failure and increasing hydration due to Na^+ ions, which resulted in the swelling, deformation and dispersion of the soil aggregates and particle movement. Accordingly, the K-values of the soils studied depended first of all on ESP; the K-values were several times higher in the fine-textured M-16 soil with low ESP than in the coarser-textured but strongly sodium saturated M-11 soil. Over a certain

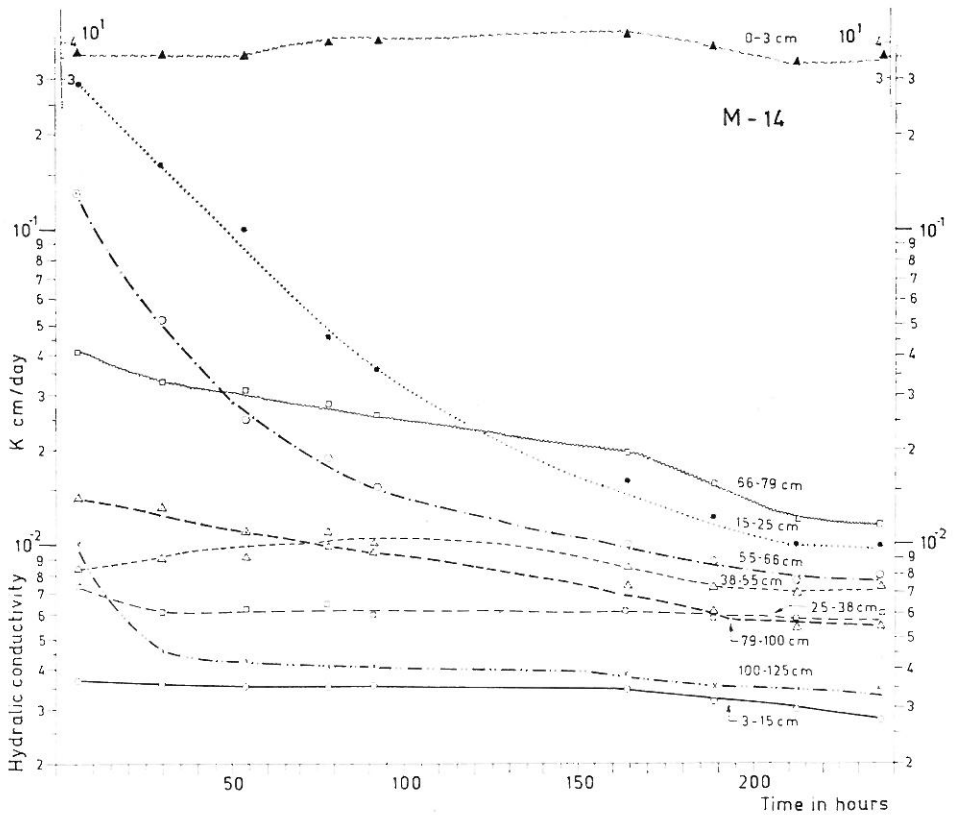

Fig. 4.11
Permability curves of a solonetz profile (saturated conductivity changes in time)

"threshold" clay content or Na^+ saturation a further increase in clay content or ESP did not affect the hydraulic conductivity. At low Na^+ saturation the K-values depended mainly on the ESP (M-16), whereas in coarse-textured soils K-values were correlated mainly with the clay content (deeper horizons of M-11). The ESP was very high in the salt affected soils studied, so the K-values were higher in the coarse-textured soda solonchak (M-11) than in the fine-textured solonetz (M-14). The hydraulic conductivity was relatively higher in the layers with a higher water soluble salt content, irrespective of salt composition.

The hydraulic conductivity of soils significantly decreased during the determination, which promoted leaching with distilled water.

Analysing the mechanism of the decrease in hydraulic conductivity, two

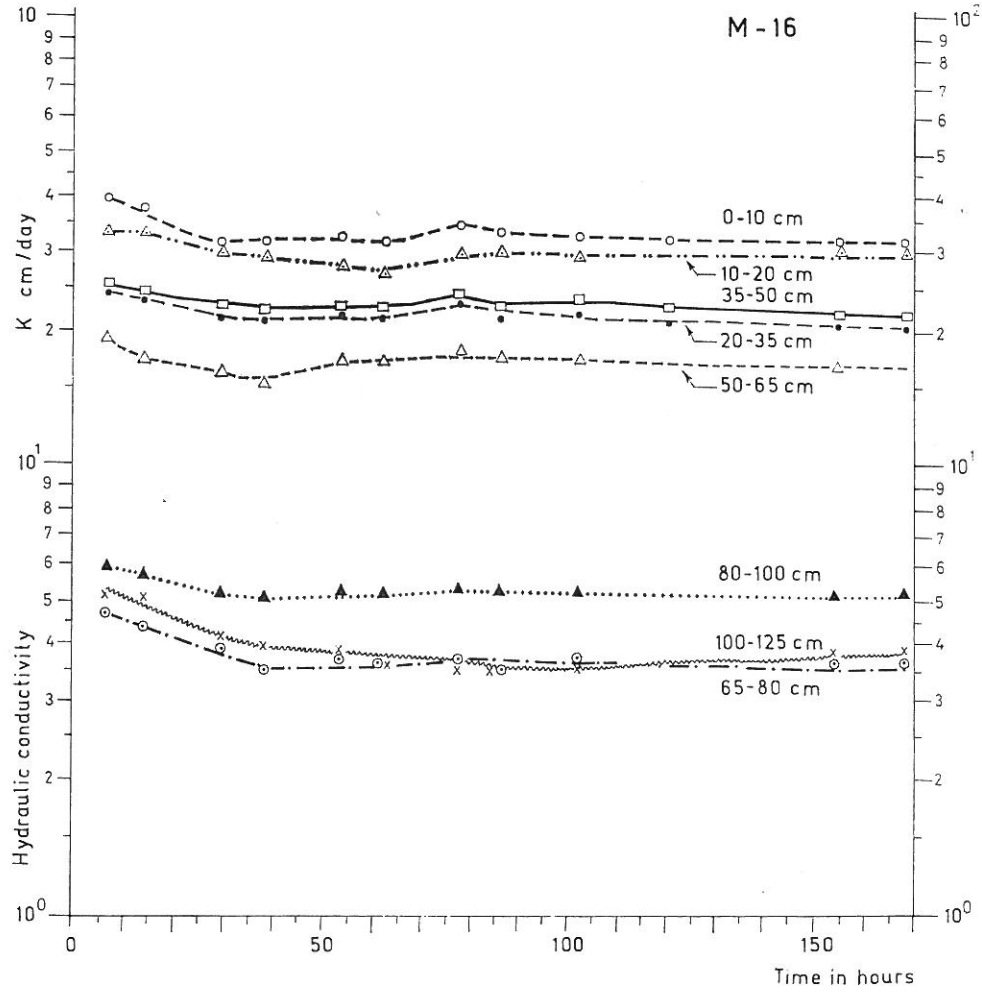

Fig. 4.12
Permeability curves of a meadow soil profile (saturated conductivity changes in time)

main types of changes can be distinguished [McNeal et al. 1968; Várallyay 1974c]:

(i) K decreases with an increase in bulk density, in accordance with the Kozeny-Carman or similar equations which express the fact that hydraulic conductivity increases proportionally with porosity [Hillel 1971, 1972]. The causes of this phenomenon are aggregate destruction and clogging of macropores by particle movement, i.e. a largely irreversible mechanical compaction.

(ii) K decreases with a decrease in bulk density.

Under the effect of the high electrolyte concentration of the soil solution a reversible flocculation of the primary particles takes place due to their low electrokinetic (zeta) potential. The floccule formed in this way is "stable" only in a certain concentration range and if the concentration decreases to below the "threshold limit", the particles, which are not cemented or bound together, will be dispersed again [McNeal et al. 1968]. Consequently, the hydraulic conductivity (K) of highly saline soils are relatively high but during leaching the electrolyte concentration of the permeating soil solution falls below the "threshold "concentration. So the flocculation effect of high salinity becomes negligible and the physical consequences of high Na^+-saturation manifest themselves more strongly. Here, besides the changes mentioned in (i), an intensive swelling takes place due to the high hydration of absorbed Na^+ ions and expanding clay minerals.

As a consequence of swelling, the bulk volume and total pore volume increase and the bulk density decreases with increasing Na^+-saturation. At the same time, the saturated hydraulic conductivity sharply decreases, as is shown in Figures 4.10 and 4.11 [Várallyay 1972, 1974c]. This phenomenon is quite contrary to what one would expect from the Kozeny-Carman or similar equations, which show that conductivity is proportional to porosity. Here, due to the high rate of dispersion and hydration, a special pore-size redistribution takes place: a considerable proportion of the water occurs in fine pores, strongly bound to the solid particles (sorption, interlayer water, etc.) and consequently cannot be removed under certain hydraulic gradients, so it shows a special "semi-solid" state. In extreme cases this semi-solid "dead water" completely fills the pores and due to this "clogging" the hydraulic conductivity can be as low as zero [International Source Book 1967; Hadas et al. 1973; Várallyay 1972, 1974c, 1978b; Water in Heavy Soils 1976]. Another consequence of the previously mentioned pore-size redistribution is the non-Darcian flow behaviour [Gardner 1960; Kirkham and Powers 1972; Kovács 1976; Nerpin and Chudnovsky 1975; Nielsen 1972; Water in the Unsaturated Zone 1968]: conductivity increases with an increasing hydraulic gradient, because in such cases an increasing part of the "semi-solid" water state can take part in the flow process.

The water retention data (Fig. 4.7) support this concept and prove that with an increase in ESP, the water retention increases and the gravitational pore space sharply decreases.

A similar mechanism was described by numerous authors [Lagerwerff et al. 1969; Lutz and Kemper 1959; McNeal 1968; Waldron and Constantin 1968] and discussed by Firemen and Bodman [1940], Waldron and Constantin [1968, 1970], McNeal and Coleman [1966], Quirk and Scofield [1955], Reeve and Tamaddoni [1965] and others.

In accordance with the results of McNeal and Coleman [1966] and McNeal et al. [1968] it was found that the K-decrease per unit volume of percolating solution was highest in the heavy textured Hortobágy solonetz (M-14).

In the first period of the observation there was a sharp decrease in the hydraulic conductivity. This was followed by a moderate decrease and after 70—170 hours the K-values became nearly constant.

The influence of various Na-solutions on the saturated hydraulic conductivity was studied in another laboratory model experiment. The experimental procedure was similar to that for the pF-determinations: The fragmented air-dry samples of Törökszentmiklós No. 349 (Meadow chernozem A-horizon, slightly calcareous clay loam) and Érd No. 169 (Pseudomyceliar chernozem A-horizon, calcareous loam) soils were uniformly packed into a 100 cm^3 brass cylinder (volume weights were 1.16 ± 0.02 g/cm^3 and 1.29 ± 0.02 g/cm^3, respectively). The soils were saturated with H_2O or with 0.05N, 0.01N and 0.5N Na_2CO_3 solutions. After saturation the saturated hydraulic conductivity (K = cm/day) was determined by the falling head method [Fig. 4.9; equation (4.19)]. Saturated hydraulic conductivity changes were registered, until they became stabilized. The data measured are summarized in Table 4.9. Some important soil characteristics (volume weight, pH, total salt content, exchangeable Na^+-content, ESP) were also determined at the end of the experiment. These results are given in Table 4.11.

For the mathematical approach to the description of saturated conductivity changes with time (K-t function) there are two possibilities:

1. Without giving a detailed analysis of the mechanisms of the existing processes, to use only empirical equations and experimentally determined constants for the characterization of each separate case.

2. To establish a synthetic mathematical model for the description of the phenomena. By solving the equation of the model the $K(t)$ relationship can be obtained directly. In this case it is necessary to distinguish and quantitatively characterize the main processes influencing the phenomena studied.

There are a lot of processes which determine or at least influence the saturated flow of soil solutions, e.g. weathering of mineral constituents, formation and transformation of clay minerals, transport of solid particles, interactions between the solid and liquid phase (dissolution and precipitation of soluble components, cation exchange, etc.). In most cases these factors result in swelling, influencing flow phenomena in this "integrated" way. Consequently, for the mathematical modelling of $K(t)$ relationships the exact and quantitative characterization of swelling properties are required.

For an approximation to the mathematical description of hydraulic conductivity changes with time an empirical formula was applied:

$$\frac{K-K_\infty}{K_0-K_\infty} = e^{-\mu t} \tag{4.20}$$

where K = saturated hydraulic conductivity at the given moment (cm/day)
K_0 = saturated hydraulic conductivity at the beginning of the experiment
K_∞ = saturated hydraulic conductivity at the equilibrium state (cm/day)
t = time (hours)
μ = experimentally determined constant

Table 4.9

Permeability curves (saturated conductivity changes in time) for Törökszentmiklós clay loam (No. 349) and Érd loam (No. 169) treated with Na_2CO_3 solutions of various concentration. Measured (M) and calculated (C) values of K = cm/day. Equation (4.20)

Soil and observation period t = hours	H_2O		Na_2CO_3									
			0.001 N		0.01 N		Observation period t = hours	0.1 N		Observation period t = hours	0.5 N	
	K = cm/day							K = cm/day			K = cm/day	
	M	C	M	C	M	C		M	C		M	C
Clay loam No 349												
0 – 2	4.29	4.237	4.16	4.124	4.29	4.203	0 – 2	0.520	0.522	0 – 2	0.049	0.050
2 – 4	3.85	3.884	3.55	3.580	3.81	3.696	2 – 4	0.216	0.205	2 – 4	0.049	0.049
4 – 6	3.59	3.584	3.14	3.162	3.13	3.266	4 – 6	0.077	0.095	4 – 18	0.050	0.047
6 – 8	3.29	3.329	2.80	2.840	2.71	2.901	6 – 8	0.063	0.056	18 – 28	0.043	0.044
8 – 12	2.94	3.017	2.49	2.492	2.40	2.456	8 – 12	0.054	0.040	28 – 44	0.040	0.041
12 – 16	2.78	2.704	2.27	2.195	2.00	2.010	12 – 28	0.049	0.036	44 – 52	0.036	0.039
16 – 20	2.41	2.478	2.13	2.022	1.72	1.690	28 – 36	0.040	0.036	52 – 68	0.039	0.037
20 – 24	2.38	2.315	1.93	1.919	1.62	1.460	36 – 52	0.040	0.036	68 – 76	0.036	0.036
24 – 28	2.32	2.197	1.87	1.858	1.57	1.294	52 – 60	0.035	0.036	76 – 92	0.036	0.035
28 – 31	2.11	2.122	1.69	1.826	1.17	1.188	60 – 76	0.033	0.036	92 – 100	0.033	0.034
31 – 36	2.05	2.058	1.59	1.803	1.11	1.099	76 – 84	0.034	0.036	100 – 164	0.034	0.032
36 – 40	1.98	2.007	1.68	1.788	0.93	1.029	84 – 148	0.033	0.036	164 – 172	0.031	0.031
40 – 44	1.91	1.976	1.91	1.781	0.87	0.985	148 – 156	0.029	0.036	172 – 188	0.032	0.030
44 – 48	1.96	1.953	1.96	1.776	0.90	0.953	156 – 172	0.030	0.036	188 – 192	0.027	0.030
							172 – 176	0.029	0.036			
Loam No 169												
0 – 10	63.7	64.2	30.6	32.4				0.068	0.067		0.064	0.061
10 – 34	58.8	58.2	29.7	28.3				0.058	0.061		0.052	0.054
34 – 58	51.1	50.7	26.0	23.5				0.055	0.058		0.044	0.047
58 – 106	41.5	41.2	16.6	18.1				0.058	0.058		0.041	0.041
106 – 154	29.7	31.4	12.2	13.4				0.056	0.058		0.039	0.036
154 – 190	24.2	24.8	11.1	10.8				0.058	0.058		0.033	0.033
190 – 216	21.9	20.9	9.6	9.4				0.058	0.058		0.040	0.033
216 – 264	17.6	171.	7.6	8.3				0.059	0.058		0.039	0.032
264 – 313	14.4	13.2	7.4	7.3				0.060	0.058		0.039	0.031
313 – 338	10.2	10.9	7.2	6.8				0.059	0.058		0.044	0.031
338 – 364	8.9	9.5	6.9	6.5				—	—		—	—

Equation (4.20) expresses the fact that the rate of the approach of K to the equilibrium (K_∞) is proportional to the current value of the deviation from the equilibrium state:

$$\frac{d}{dt}(K - K_\infty) = -\mu(K - K_\infty) \tag{4.21}$$

which means that the K-decrease can be described by a kinetic equation of the first order.

The results of approximations with equation (4.20) are shown in Figures 4.13 and 4.14, and the data are summarized in Table 4.9. The constants K_0, K_∞ and μ are given in Table 4.10. There was good agreement between the measured

Table 4.10

Experimentally determined parameters of equation (4.20) applied for the description of permeability curves (changes of saturated conductivity in time)

Soil (Code No) and solution	K_0	K_∞	μ	Soil (Code No) and solution	K_0	K_∞	μ
349				**169**			
H_2O	4.436	1.893	0.0817	H_2O	66.120	8.510	0.00593
Na_2CO_3				Na_2CO_3			
0.001 N	4.455	1.770	0.1313	0.001 N	33.810	5.681	0.00993
0.01 N	4.489	0.872	0.0826				
0.1 N	0.860	0.0363	0.5278	0.1 N	0.0703	0.0576	0.06363
0.5 N	0.050	0.0292	0.0158	0.5 N	0.0636	0.0310	0.01504

data and the calculated values (mean standard deviation was not more than 10%). In most cases K decreased with an increasing concentration of Na_2CO_3. μ does not give a monotonous dependence from Na_2CO_3 concentration because it is affected by other factors (soil characteristics, chemical composition of the filtrating solution, etc.), as well.

The possibility of approximating the $K(t)$ relation by equation (4.20), using the constant μ, means that the factors which play a role in the K-decrease with time did not change during the experiment.

As can be seen from the measured data the tendency and character of hydraulic conductivity changes are similar to those discussed previously:

1. K-values decrease even under the influence of distilled water leaching, especially in Érd loam, where the well-developed aggregation results in high initial conductivity values but the aggregate stability proved to be rather poor. In these cases the K-decrease was primarily the combined consequence of a more or less irreversible mechanical compaction (structure destruction, aggregate failure, dispersion, peptization, clogging of macropores by particle movement, etc.) and a moderate swelling (which was not prevented as in the pF-measurements).

2. Under the influence of Na_2CO_3 solutions the hydraulic conductivity decreased sharply with increasing solute concentration ($\rightarrow$ increasing ESP: Table 4.11), especially at concentrations above 0.1N ($\approx$ ESP 30), where the

Table 4.11

The influence of Na_2CO_3 solutions of various concentration on some soil properties in the saturated flow experiment

Soil (Code No) and solution	pH	Bulk density g/cm³	ESP	Total soluble salt content %	Soil (Code No) and solution	pH	Bulk density g/cm³	ESP	Total soluble salt content %
349					**169**				
Original soil	6.9	1.16	0.2	0.05	Origina soil	7.7	1.29	0.1	0.03
H_2O	6.8	1.15	0.2	0.03	H_2O	7.5	1.34	0.1	0.02
Na_2CO_3					Na_2CO_3				
0.001 N	7.2	1.14	1.4	0.07	0.001 N	7.8	1.27	8.6	0.09
0.01 N	7.9	1.13	8.3	0.10					
0.1 N	8.7	1.07	30.0	0.21	0.1 N	8.8	1.10	32.1	0.19
0.5 N	9.7	0.90	68.2	1.10	0.5 N	9.9	0.97	61.1	1.04

soils became practically impermeable, due to the combined influences of desaggregation, particle movement and swelling (→ high rate of hydration → considerable amount of "semi-solid state" water and its "clogging effect").

As a general conclusion it can be stated that in $NaCl-Na_2SO_4$ type salt affected soils (salinization caused by neutral sodium salts) the influence of relatively low Na^+ saturation can be counter-balanced by the flocculation

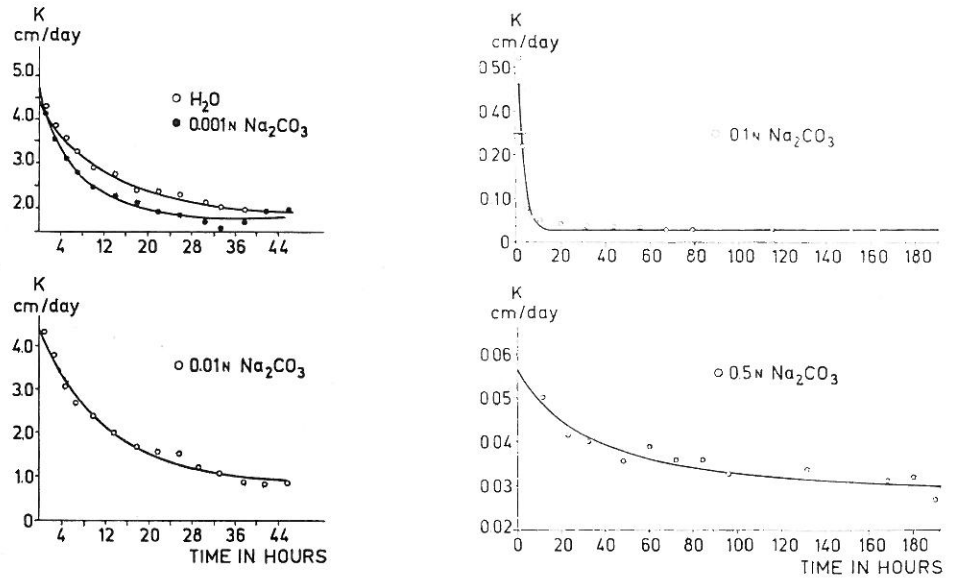

Fig. 4.13

Permeability curves (saturated hydraulic conductivity changes in time) for Törökszentmiklós clay loam (No 349) treated with Na_2CO_3 solutions of various concentration. The points are the measured values; the curves were calculated with equation (4.20)

effect of high salinity; consequently, these soils have relatively better permeability. By contrast, the hydraulic conductivity of heavy-textured, soda-salinized alkali soils decreases sharply with an increase in ESP (Table 4.9) [VÁRALLYAY 1972, 1974c, 1977, 1978b].

Because of the extremely low vertical and horizontal saturated hydraulic conductivity of heavy-textured, swelling clay-containing alkali soils, their natural drainage is very poor, and the possibilities of leaching are limited. Consequently, their formation processes, caused by sodium salts capable of alkaline hydrolysis are almost irreversible [KOVDA 1974; SZABOLCS 1969, 1971a, 1974; VÁRALLYAY and SZABOLCS 1974, 1978].

The key problem in the agricultural utilization of heavy-textured soda soils, apart from the control of saline ground water [TALSMA 1963] is the improvement and maintenance of sufficient permeability to permit salinity control and reclamation. For the amelioration of these soils leaching (irrigation and drainage) alone is not sufficient because it may result in a reverse effect (diluted solutions → decrease in permeability). Therefore, leaching has to be combined with the application of chemical amendments (gypsum, etc.) and proper tillage practice. Because these complex ameliorative measures are rather expensive, in these soils the p r e v e n t i o n of salinization and alkalization has special importance and sometimes this is the only way (at least the only economic way) to maintain the soil properties within a range required for proper agricultural production [DARAB, SZABOLCS and VÁRALLYAY 1973; International Source Book 1967; Prognosis of Salinity and Alkalinity 1975; SZABOLCS, DARAB and VÁRALLYAY 1972, 1976; VÁRALLYAY 1968; WORTHINGTON 1977].

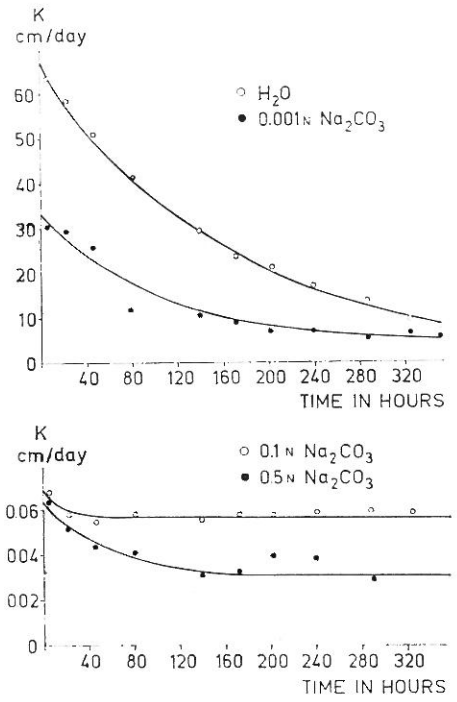

Fig. 4.14
Permeability curves (saturated hydraulic conductivity changes in time) for Érd loam (No 169) treated with Na_2CO_3 solutions of various concentration. The points are the measured values; the curves were calculated with equation (4.20)

The various mechanisms responsible for solute movement in soils (diffusion, convection or viscous flow and combinations of these, hydrodynamic dispersion, miscible displacement, salt sieving effect, etc.) have been accurately analysed by numerous authors [BEAR, ZASLAVSKY and IRMAY 1968; CHILDS 1969; HADAS et al. 1973; HILLEL 1971; KIRKHAM and POWERS 1972; NERPIN and CHUDNOVSKY 1967, 1975; NIELSEN 1972; PHILIP 1972; YONG and WARKENTIN 1975] but these problems are not included in the present chapter.

4.3. Salinity-alkalinity and liquid flow in the unsaturated zone

Liquid flow processes of the field water cycle, taking place within the soil profile between the soil surface and the water table (infiltration, vertical and horizontal moisture redistribution, diffusion, upward capillary flow from the ground water, liquid flow to the plant roots, etc.) are typical cases of unsaturated flow phenomena. These processes have wide practical importance for agriculture and particular significance under saline and alkali conditions:

— in most cases the limiting factors of the fertility of salt affected soils are their unfavourable water physical properties and the inadequate water supply to the plants,

— in many cases the water soluble salts — responsible for the salinity and alkalinity of soils — are accumulated from the ground water [DARAB and FERENCZ 1969; KOVDA 1937, 1947, 1954, 1965; MORGUN 1976; Proc. Symp. ISSS Subcomm. 1965, 1969, 1975; Prognosis . . . 1976; Salinity Problems . . . 1961; International Source Book 1967, SZABOLCS 1961; SZABOLCS, DARAB and VÁRALLYAY 1969, 1972, 1976; TALSMA 1963; VÁRALLYAY 1968; WORTHINGTON 1977].

For the description of water movement in the unsaturated zone the general mass-flow equation can be applied in a differential form:

$$\frac{\partial \theta^*}{\partial t} = -\frac{\partial V}{\partial x} - I_\theta \tag{4.22}$$

where $\theta^* =$ water filled pore volume (cm^3/cm^3)
$I_\theta =$ volume of water removed from unit volume of soil per unit of time (hydration, evaporation, water uptake by plant)
$V =$ volume of water flow through a unit cross-section per unit of time in the direction of the x axis (vertical upward)

The problem of the redistribution of water cannot be solved using only equation (4.22), because in this equation there are three unknown parameters: θ^*, V and I_θ. Consequently, at least two more equations have to be obtained. For this purpose unsaturated hydraulic conductivity and suction were determined, then using the DARCY formula and the empirical relations $k = k(\psi)$; $\theta = \theta(k)$; and assuming that $I_\theta = 0$, a system can be obtained consisting of four equations for the four unknown parameters: θ^*, V, k, ψ.

The unsaturated flow dependence of the gradient of the total driving force and unsaturated (capillary) conductivity may be expressed as:

$$V = -K \cdot \operatorname{grad} \psi_t \tag{4.23}$$

Substituting equation (4.1) instead of ψ_t this gives:

$$V = -k \cdot (\operatorname{grad} \psi_g + \operatorname{grad} \psi_p + \operatorname{grad} \psi_s) \tag{4.24}$$

In the case of isothermal steady-state unsaturated flow in soils ψ_s and ψ_p^a can be neglected, therefore:

$$V = -k(\operatorname{grad} \psi_g + \operatorname{grad} \psi) \tag{4.25}$$

Two important differences have to be recognized between saturated and unsaturated flow:

1. The moving force resulting from the gradient of the hydraulic pressure is replaced by a pulling force, mainly by the gradient of the matric potential (grad $\psi = \Delta\psi/\Delta z$).

2. The cross-section through which the water flows is reduced when the pores are only partially filled with water. As a consequence of this, the hydraulic conductivity of unsaturated soils (capillary conductivity, k = cm/day) cannot be characterized by a single value but only as a function of suction or moisture content, and the capillary conductivity is always lower than the saturated hydraulic conductivity ($k < K$). The water-filled pore volume at a certain suction is reflected by the water retention (pF) curves. It is obvious that with an increase in suction there is a decrease in moisture content, in water-filled pore volume and, consequently, in capillary conductivity as well [BAVER, GARDNER and GARDNER 1972; VÁRALLYAY 1974a, 1978b].

Accordingly, the general unsaturated flow equation can be written as follows:

$$V = k \cdot \left[\frac{\Delta\psi}{\Delta z} - \psi_g \right] \tag{4.26}$$

where V = vertical flow velocity, cm/day
k = capillary conductivity, cm/day
ψ = matric potential (suction), cm
Δz = height above a certain reference level, cm
$\Delta\psi/\Delta z$ = suction gradient, cm/cm
ψ_g = potential due to gravity (≈ 1).

The relation between capillary conductivity and suction can be determined by field and laboratory methods. WIND [1961] and TALSMA [1963] calculated this $k = f(\psi)$ or $k = f(\theta)$ relationship from field measurements of the changes in the moisture (or suction) profiles of soils, recorded by tensiometers installed at various depths. GARDNER [1956], MILLER and ELRICK [1958], RIJTEMA [1959] and others [JACKSON, BAVEL and REGINATO 1963] calculated capillary conductivity from pressure-membrane outflow data [BAVER, GARDNER and GARDNER 1972]. After STAPLE and LEHANE [1954] many authors computed the non-steady state and steady-state capillary flow from the moisture profile redistribution in disturbed or undisturbed soil columns or from the equilibrium moisture profile resulting from a certain constant suction gradient. In this relation the use of γ-radiation techniques offers new possibilities [BOODT et al. 1973; NERPIN and HLOPOTENKOV 1971; OLSZTA 1975; Water in the Unsaturated Zone 1968]. RICHARDS [1965], RICHARDS and MOORE as well as KLUTE [In: Methods of Soil Analysis 1965], NIELSEN [1972] and others measured capillary conductivity as a function of suction in a special apparatus [BUTIJN and WESSELING 1959; GLOBUS 1969].

Based on the laboratory infiltration method of CHILDS and COLLINS-GEORGE [1950] and WESSELING and WIT [1968] apparatuses were constructed for the determination of the $k = f(\psi)$ relationship under steady-state conditions [VÁRALLYAY 1974a].

These apparatuses are schematically illustrated in Figures 4.15, 4.16 and 4.17. This method can be used primarily on light-textured soils in the low suction range ($\psi = 0-500$ cm). During the measurements a constant flux (V = cm/day) is established through a vertical undisturbed soil column by precisely controlled and stabilized infiltration, using various accurate

feeding systems. The existing suction gradient $\frac{\Delta\psi}{\Delta z}$ in the soil column is continuously measured, registering the suction (ψ = cm) at 10 cm intervals (z = 10 cm) by small, sintered glass tensiometers placed in the soil column. At equilibrium the capillary conductivity is computed with equation (4.26) which, solving for k, gives:

$$k = \frac{V}{\frac{\Delta\psi}{\Delta z} - 1} \tag{4.27}$$

Repeating the same procedure at various flow velocities and suctions (precisely controlled by suction plates) an adequate amount of data can be obtained for the quantitative characterization of the $k - \psi$-relationships [CHILDS and COLLINS-GEORGE 1950; VÁRALLYAY 1974a; WESSELING and WIT 1968].

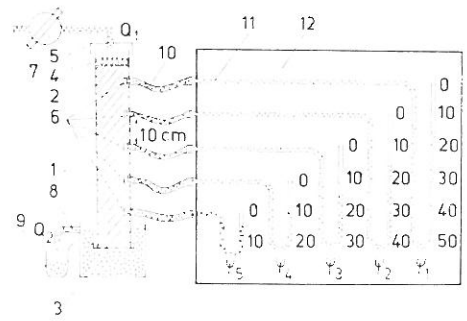

Fig. 4.15
Apparatus for the laboratory determination of capillary conductivity in the $\psi = 0-50$ cm suction range. 1. PVC cylinder with circular holes (10 mm in diameter) on one side at 10 cm intervals. 2. Undisturbed soil column. 3. Nylon cloth attached to the lower opening of the PVC cylinder with a rubber band. 4. Sponge disc, for the uniform distribution of the infiltrating liquid. 5. Lid, closing the upper opening of the PVC cylinder, to prevent evaporation. 6. Tensiometers: 1.5 mm thick, sintered glass plates, 6 mm in diameter, mounted into a glass tube. 7. Precision feeding system. 8. Constant-level vessel with overflow. 9. Collecting vessel. 10. Transparent plastic tubing. 11. Water-filled manometers. 12. Manometer panel

In the high suction range ($\psi >> 500$ cm) the evaporation column procedure was applied. This is based on the continuous or periodical registration of moisture profile redistribution which was first suggested by STAPLE and LEHANE [1954], modified by WIND [1968] and adopted for cases when a water table is present by DIESTEL [1974], KUTILEK [1973] and others [ARYA 1973; HILLEL 1971; OLSZTA 1975; Water in the Unsaturated Zone 1968]. In our experiment the modified WIND procedure [1968] was applied, using 11 cm long, uniformly packed (density 1.29 g/cm^3), homogeneous soil columns. The consecutive steps of the experiment were as follows:

(i) full saturation with water (or solutions): $\psi = 0$ within the whole column;

(ii) stabilization of water level at the lower end of the column: after equilibrium $\psi = 0$ at the bottom and $\psi = 11$ cm at the top of the column (= lower part of the pF-curve) and there is no downward flow due to gravity within the column;

(iii) closing the lower end of the column, and leaving it to evaporate in a small climatic chamber and registering the moisture profile redistribution in the column, at 1 cm intervals.

The data of these measurements are shown in Figure 4.18. Flow velocities (V) were computed from these curves, as well as from suction gradients ($\Delta\psi/\Delta z$)

using corrected pF curves [WIND 1968]. Capillary conductivity (k) as a function of suction was calculated using equation (4.27).

The measured k values may be plotted against suction on log-log paper and the function $k = f(\psi)$ can be described mathematically by using one of the following equations:

$$k = \frac{a}{\psi^n} \quad \text{[WIND 1961; WISSER 1963]} \tag{4.28}$$

where k = capillary conductivity (cm/day)
ψ = suction (water column cm)
a = experimentally determined constant (according to Visser it is related to the conductivity of nearly saturated soil)
n = experimentally determined exponent (1.5—2.0 in clay soils, higher values in sandy soils).

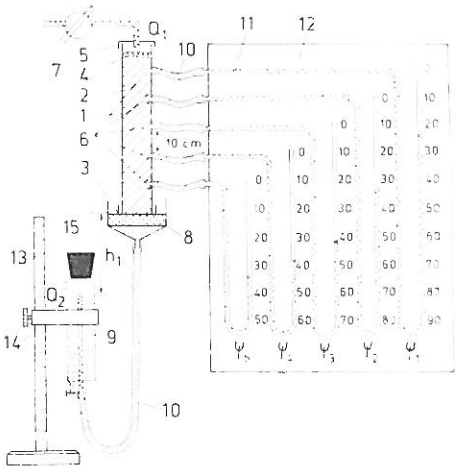

Fig. 4.16
Apparatus for the laboratory determination of capillary conductivity in the $\psi = 50$—100 cm suction range. 1—7 as in Figure 4.15. 8. Porous medium: 2—3 cm thick fine sand (air bubbling value: $\psi_a = 140$—150 cm) layer on a large pore-size, sintered glass filter-funnel. 9. Collecting vessel with a constant level tube for "hanging water column"-type vacuum regulation and stabilization $\psi_{cm} = h_1$ cm. 10. Transparent plastic tubing. 11. Water-filled manometers. 12. Manometer panel. 13. Stainless steel sliding measuring stand with cm graduation. 14. Clamp, supporting the constant-level vessel, it can be moved and fixed on the measuring stand with a screw. 15. Rubber stopper

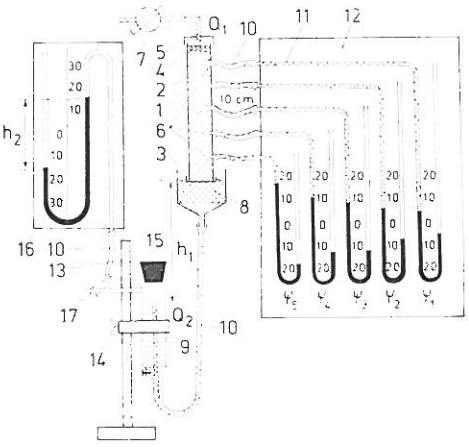

Fig. 4.17
Apparatus for the laboratory determination of capillary conductivity in the $\psi = 100$—800 cm suction range. 1—7. as in Figure 4.15. 8. Porous medium: 4—5 cm thick 1 : 2 fine sand—kaolin mixture (air bubbling value: $\psi_a = 900$ cm) layer on a large pore-size sintered glass filter-funnel. 9. Collecting vessel (at the same time depression vessel) with a constant level tube. Total vacuum is the sum of the height of the hanging water column and the depression in the vessel, registered by the mercury manometer (16): $\psi_{cm} = h_1$ cm $+ 13.5 h_2$ cm. 10. and 12. as in Figure 4.15. 11. Mercury manometers. 13—15. as in Figure 4.16. 16. Mercury manometer. 17. Glass-tubing with two stopcocks for connections to the automatic mercury vacuum stabilizer and to the mercury manometer (16).

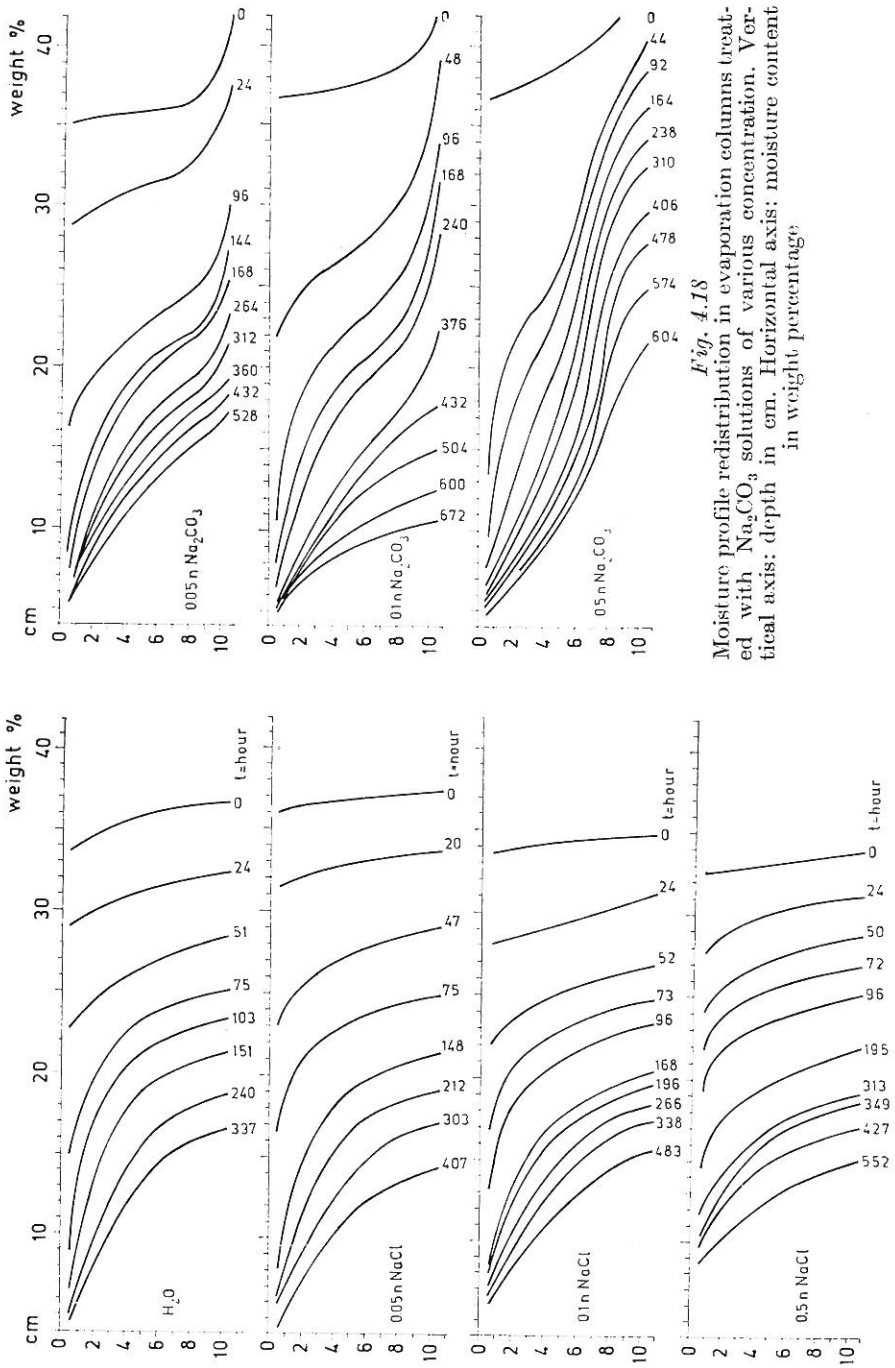

Fig. 4.18
Moisture profile redistribution in evaporation columns treated with Na_2CO_3 solutions of various concentration. Vertical axis: depth in cm. Horizontal axis: moisture content in weight percentage

$$k = \frac{a}{b + \psi^n} \quad \text{[GARDNER 1956, 1958, 1960]} \tag{4.29}$$

where k, ψ, n = see equation (4.28)
a, b = experimentally determined constants
$a/b \approx$ saturated conductivity ($\psi = 0$ cm) (cm/day)

$$k = \frac{K}{e^{\alpha(\psi - \psi_a)}} \quad \text{[RIJTEMA 1965]} \tag{4.30}$$

where k, ψ = see equation (4.28)
K = saturated conductivity (cm/day)
ψ_a = suction at the air entry point (water column cm)
α = experimentally determined constant.

The RIJTEMA equation (4.30) holds until ψ_{max} which is quite different in various soils (80 – 300 cm). In the higher suction range equation (4.28) and equation (4.29) are more suitable.

The most important practical applications of the unsaturated flow theory are:

– infiltration studies [BEAR, ZASLAVSKY and IRMAY 1968; BOODT et al. 1973; CHILDS 1969; FRISSEL and REININGER 1974; GARDNER 1960; HILLEL 1977; KIRKHAM and POWERS 1972; KOVÁCS 1976; NERPIN and CHUDNOVSKY 1975; NIELSEN 1972; Water in Heavy Soils 1976; Water in the Unsaturated Zone 1968; WIEST 1969; YONG and WARKENTIN 1975].

– determination of possibilities for water supply of plants from the ground water [ARYA 1973; BAVER, GARDNER and GARDNER 1972; DIESTEL 1974; HILLEL 1972; OLSZTA 1975; RIJTEMA 1965, 1968; ROSE 1966; Soil Physical Conditions 1975; VÁRALLYAY 1974a; WISSER 1963]

– description and prediction of salt accumulation processes from the ground water [DIESTEL 1974; FRISSEL and REININGER 1974; GARDNER 1960; HADAS et al. 1973; International Source Book 1967; PACHEPSKY et al. 1976; Proc. Symp. ISSS Subcomm. 1965, 1969, 1975; Salinity Problems . . . 1961; SOKOLENKO et al. 1976; SZABOLCS, DARAB and VÁRALLYAY 1969, 1972, 1976; TALSMA 1963; VÁRALLYAY 1974a, 1974b, 1975, 1978b, 1978d; WIT and KEULEN 1972; WORTHINGTON 1977].

For the quantitative determination of the amount of water and salts entering the soil profile from the ground water a method was elaborated by VÁRALLYAY [1974a, 1974b, 1975, 1978b, 1978d] with the application of the unsaturated flow theory.

This hydrophysical approach gave more exact and quantitative data for the prediction of salinization and alkalization processes and it was built into the system for the salinity-alkalinity prognosis suggested by the FAO Expert Consultation and elaborated in international cooperation [1976].

The hydrophysical approach includes four main steps:

1. Determination of unsaturated hydraulic conductivity as a function of suction ($k - \psi$ or $k - \theta$) relationship. The unsaturated conductivity as a function of suction was determined by the infiltration [CHILDS and COLLINS-GEORGE 1950; VÁRALLYAY 1974b; WESSELING and WIT 1968] and evaporation [WIND 1968] methods in the lower and higher suction ranges, respectively and

the $k - \psi$ relationship was described by the GARDNER-equation (4.29) [GARDNER 1958, 1960]. The measured $k = f(\psi)$ relations are illustrated for four soils in Figure 4.19 and the experimentally determined a, b and n parameters of equation (4.29) are given below:

No.	a	b	n
196	182	150	1.70
198	5600	5600	2.50
191	$3.17 \cdot 10^5$	$1.0 \cdot 10^4$	2.65
301	$8.0 \cdot 10^7$	$8.0 \cdot 10^5$	4.50

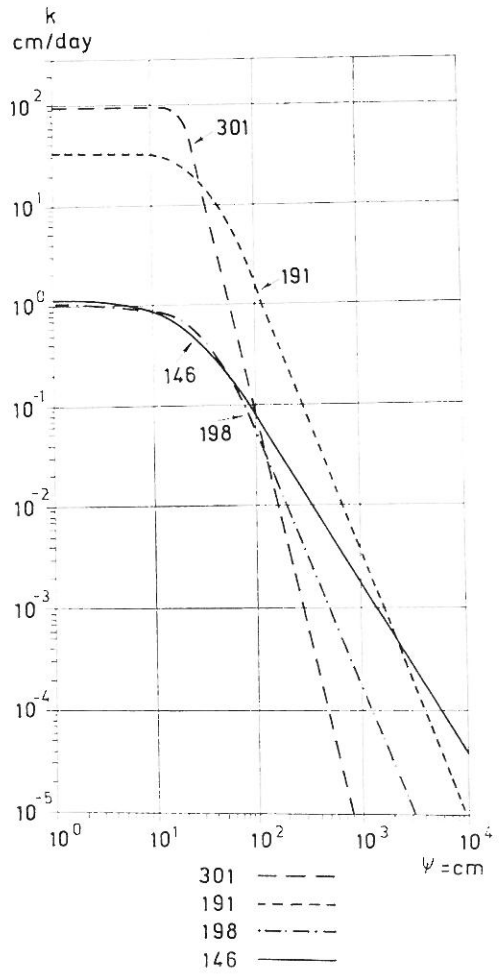

Fig. 4.19
Relation between capillary conductivity (k = cm/day) and suction (ψ = cm) for the soils studied

In the low suction range k is higher in coarse-textured or well aggregated soils, because their large pores are nearly saturated. This is reflected by the pF-curves (Table 4.2, Fig. 4.6). The water-filled pore volume, and consequently k, decreases with increasing suction, particularly in coarse-textured soils, where the volume of fine pores is not significant. At pF 2.0 k is similar in the various soils studied and in the high suction range k-values are higher in fine textured soils, because a considerable portion of their finer pores are filled with water even under higher suction. Above pF 3.5 – 4.2 liquid flow is practically negligible [BAVER, GARDNER and GARDNER 1972; BOODT et al. 1973; HILLEL 1971; KIRKHAM and POWERS 1972; NIELSEN 1972].

2. The vertical flow of water through a homogeneous soil profile can be characterized by the application of the simplified unsaturated flow equation (4.26). With integration and solving for "z" equation (4.26) gives:

$$z = \int_0^{\psi} \frac{d\psi}{1 + V/k} \qquad (4.31)$$

where z is the vertical distance above the water table. Based on the experimentally measured $k = f(\psi)$ relationship (Fig. 4.19), with the application of equation (4.31) a special type of curve sets can be constructed, expressing and clearly indicating the direction of vertical capillary flow and the velocity of upward flow (V = cm/day) as a function of the suction profile (ψ = water column cm) and the height above the water table (z = cm) [RIJTEMA 1965, 1968; TALSMA

1963; VÁRALLYAY 1974a, 1974b, 1978d; WIND 1961]. The curve sets are presented for some studied soils in Figure 4.20. It follows from equation (4.31) and can be seen from the curve sets (Fig. 4.20) that as long as the suction (ψ = water column centimetres) at the soil surface (or at a certain depth in the soil

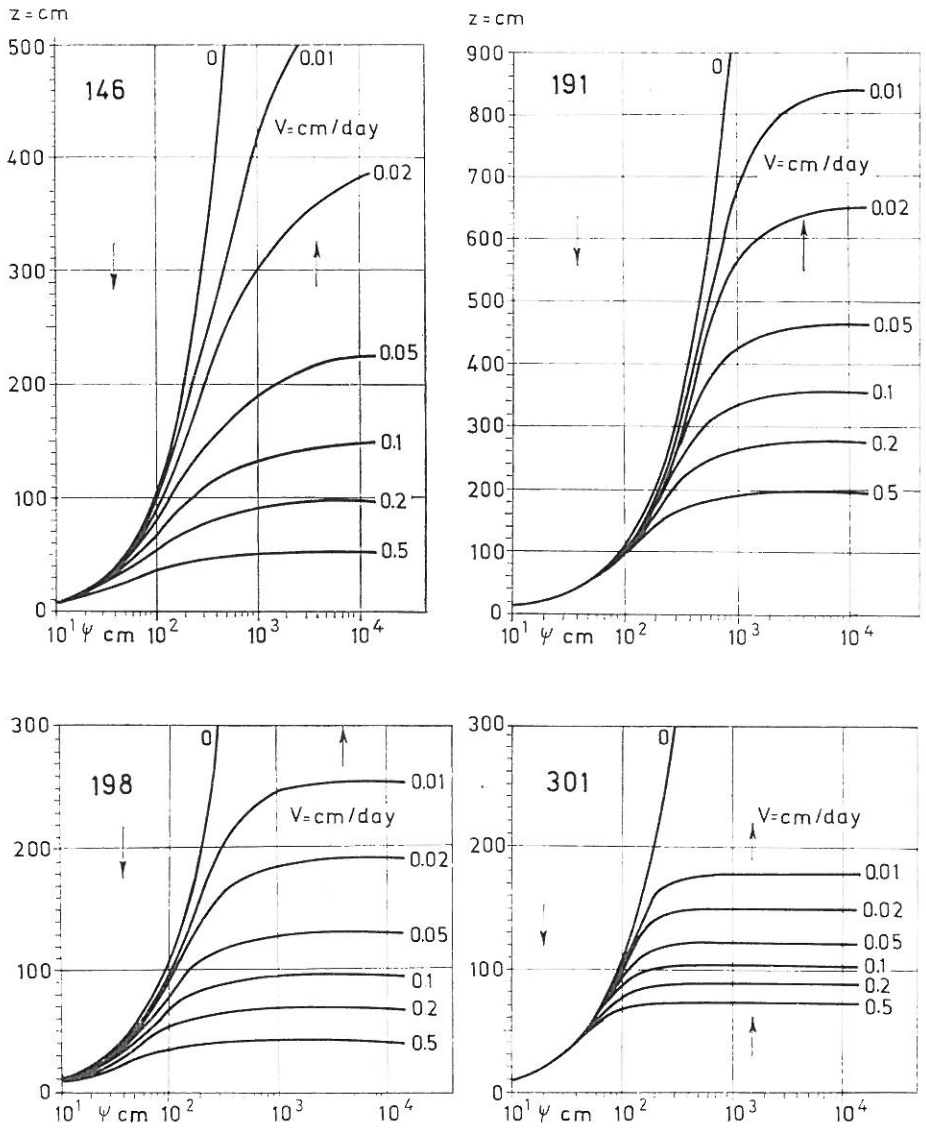

Fig. 4.20
The direction of vertical capillary flow and the velocity of upward capillary flow (V = = cm/day) as a function of the height above the water table (z = cm) and suction (ψ = cm) in the studied soils

profile) is greater than the depth to the water table (or the height of this point above the water table: z = cm), $\psi > z$, water will move upwards. If $\psi = z$ (equilibrium condition) there is no capillary flow. If $\psi < z$ there is a downward capillary flow (Fig. 4.20) [GARDNER, 1960].

The velocity of upward capillary flow (V = cm/day) depends on the capillary conductivity at the given suction (k = cm/day) and on the suction gradient $\frac{\Delta\psi}{\Delta z}$, as follows from equation (4.26). Because capillary conductivity is a function of suction (ψ = cm), which is dependent on the vertical distance above the water table (z = cm), therefore the velocity of upward capillary flow depends to a great extent on the height above the water table, especially in coarse-textured soils where k decreases sharply with increasing suction (Fig. 4.20).

In coarse-textured soils V sharply decreases with increasing z and is practically independent of ψ: capillary flow transports considerable amounts of water (and water soluble salts) from a shallow ground water to the overlying horizons, while this quantity is negligible in the case of a deep water table. In finer-textured soils V only decreases moderately with increasing z and depends to a high extent on the suction profile (Fig. 4.20): capillary flow transports relatively large quantities of water (and soluble salts) even from a deep ground water to the overlying horizons, especially in the case of a high suction gradient [GARDNER 1969; TALSMA 1963].

3. For layered soil profiles the maximum upward capillary flow velocities (as a function of suction) at a given height above the water table can be determined only by an integrated analysis of the $k = f(\psi)$ relationship (Fig. 4.19), or by using the characteristic set of curves (Fig. 4.20) for the consecutive layers [WIND 1961]. V depends largely on k and on the thickness and sequence of the horizons in the soil profile. If the texture becomes coarser with depth (clay on sand: typical alluvial sedimentation) the upward capillary flux increases because both the clay in the high suction range (far from the water table) and the sand in the low suction range (near to the water table) have relatively high k values. If the texture becomes heavier with depth (sand on clay) the upward capillary transport is moderated because both the clay in the low suction range and the sand in the high suction range have relatively low unsaturated conductivity [WIND 1961].

Our data support the statement of several authors [DIESTEL 1974; GARDNER 1960; International Source Book 1967; KOVDA 1947, 1965; MORGUN 1976; OLSZTA 1975; Proc. Symp. ISSS Subcomm. 1965, 1969, 1975; Salinity Problems ... 1961; SZABOLCS 1965, 1970, 1971a, 1974; TALSMA 1963; VÁRALLYAY 1968, 1974b, 1977, 1978b; VÁRALLYAY and SZABOLCS 1974, 1978; WORTHINGTON 1977] that the capillary flow transports considerable amounts of water (and soluble salts) even from a relatively deep ground water to the overlying horizons, particularly in moderately heavy-textured soils and in soil profiles where the texture becomes heavier with depth (alluvial stratification). These conditions are favourable for the water supply of plants from the ground water (in the case of fresh ground water and properly controlled drainage) [ARYA 1973; OLSZTA 1975; RIJTEMA 1965, 1968; Soil Physical Condition ... 1975; Water in the Unsaturated Zone 1968; WIND 1961; WISSER 1963], but they are also favourable for salt accumulation in soils from the ground water

(in the case of saline, stagnant ground water and improper drainage) [DIESTEL 1974; GARDNER 1960; International Source Book 1967; KOVDA 1947; MORGUN 1976; PACHEPSKY et al. 1976; SZABOLCS 1965, 1970, 1974; TALSMA 1963; VÁRALLYAY 1968, 1977; WORTHINGTON 1977].

4. In the case of a rising or fluctuating water table the stratification of a natural soil profile changes as a result of the change in the unsaturated cross-section of the soil between the soil surface and the water table. In Figure 4.21 two schematic soil profile models are illustrated, their stratification and the rising water table are indicated. Between the soil surface and the rising water table an infinite number of variously stratified soil profiles can theoretically be distinguished. Using the above-mentioned calculation procedure computations were made for these profiles to determine the height above the water table where 0.5, 0.1 and 0.02 cm/day upward capillary flow velocities may exist (assuming again that on the soil surface $\psi = 10^{4.2}$ cm). With these calculations an adequate number of $z_{0.5}$, $z_{0.1}$ and $z_{0.02}$ values can be produced and from the $z_{0.5}$, $z_{0.1}$ and $z_{0.02}$ points$z_{0.5}$, $z_{0.1}$ and $z_{0.02}$ curves can be constructed as is illustrated in Figure 4.21.

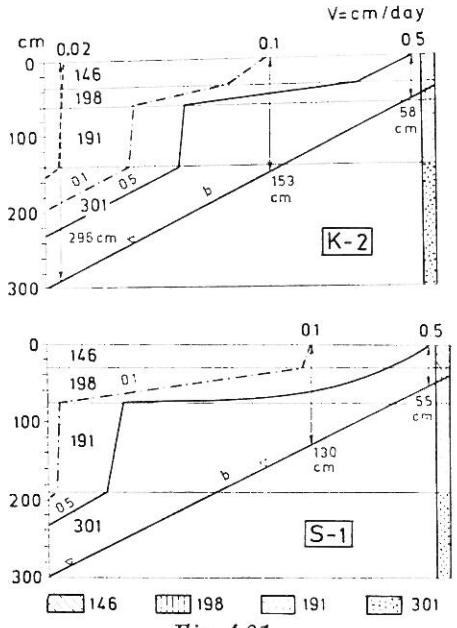

Fig. 4.21
Relation between the depth to the water table (z = cm) and the maximum upward capillary flow velocity (V = cm/day) in layered soil profile models with rising water table ($\psi = 10^{4.2}$cm)

With the application of the step by step approach summarized above, on the basis of directly measured or computed data for the time and territorial distribution of suction (or moisture) profiles in soils, the direction and velocity of vertical capillary flow in the unsaturated soil layers between the soil surface and the water table can be determined and interpreted for soil profiles, mapping units or territories. By using forecasted values instead of measured ones (from the meteorological and hydrogeological prognosis, irrigation plans) a more or less accurate prognosis can be given for the water movement in layered, unsaturated soil profiles with a fluctuating water table, and the quantity of water entering the soil profile from the ground water can be forecasted as well.

As a first approximation, disregarding the chemical and physico-chemical aspects (differences between the flow of water and solutions; interactions between the solid and liquid phases of the soils, etc.) [CHURAEV, PASHNEV and GOROKHOV 1967; DARAB 1965, 1974; FILEP 1972a, HADAS et al. 1973; International Source Book 1967; KOVDA 1947, 1965; KUTILEK 1973; MCNEAL et al. 1968; NIELSEN 1962; SZABOLCS 1969], salt transport in the soil profile and salt accumulation in the soil from the ground water can be described and/or

forecasted on the basis of water flow (discussed above) and the measured, calculated or predicted concentration and chemical composition of the filtrating solution

$$V_{salt} = [V_{water} \cdot C_{solution}] \cdot 10^{-3} \qquad (4.32)$$

where V_{salt} = net influx of salts from the ground water to the overlying soil horizons (t/ha/year)
V_{water} = net influx of water from the ground water to the overlying horizons (t/ha/year)
$C_{solution}$ = average concentration of the filtrating solution (g/lit)

This rough estimation is valid only for ideal cases. In natural soil-water-salt systems the differences between the water and solution flow (due to the reversible and irreversible, direct and indirect influences of the concentration and ion composition of the filtrating solution, and to the interactions between

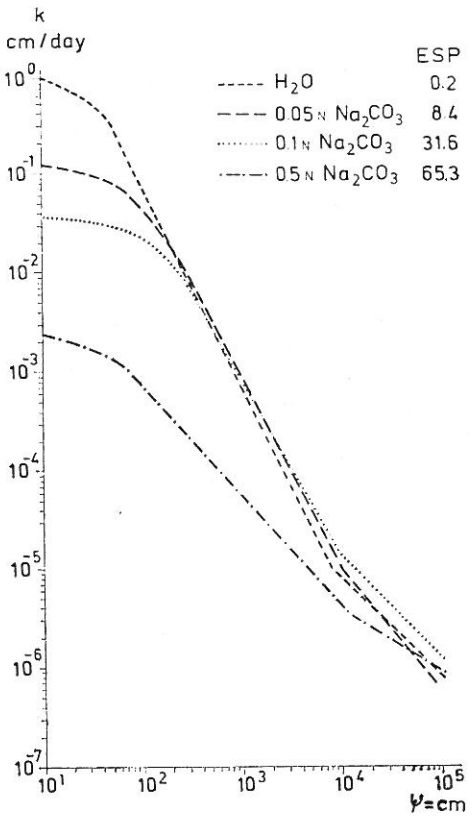

Fig. 4.22
Relation between capillary conductivity (k = cm/day) and suction (ψ = cm) in a loam (No 146) under the influence of Na_2CO_3 solutions of various concentration

Table 4.12

Relation between capillary conductivity (k = cm/day) and suction (ψ = cm) in a loam (No 146) under the influence of various Na-solutions

Suction range	Parameters	Treatment						
		H_2O	NaCl			Na_2CO_3		
			0.05 N	0.1 N	0.5 N	0.05 N	0.1 N	0.5 N
0	K	1.04	0.96	0.78	1.24	1.12	0.036	0.0026
A	ψ	< 80	< 120	< 150	< 200	< 200	< 300	< 200
	a	1751	315	529	1055	100	49.9	0.630
	b	1638	326	681	848	832	1361	246
	n	2.20	1.70	1.80	1.90	1.60	1.50	1.40
B	a	648	570	1343	1418	483	205	0.121
	n	2.00	1.88	1.99	1.96	1.92	1.80	1.11
C	ψ	> 770	> 16 000	< 16 000	< 14 000	< 8500	> 9000	> 12 000
	a	0.0978	0.431	0.786	0.465	0.766	0.201	0.0014
	n	1.01	1.13	1.21	1.12	1.21	1.03	0.63
ESP		0.2	3.9	5.6	27.6	8.4	31.6	65.3

Suction ranges: 0 = 0
A = low suction range: equation (4.29)
B = medium, C = high } suction range: equation (4.28)

the solid and liquid phases of the soils) have to be taken into consideration for the quantitative characterization of salt transport (See above).

Only few data are available in the literature on the influence of salinity and/or alkalinity on the unsaturated flow [DIESTEL 1974; HADAS et al. 1973; HILLEL 1971; NIELSEN 1972; VÁRALLYAY 1976a; Water in Heavy Soils 1976; Water in the Unsaturated Zone 1968].

For illustration of the particular importance of the chemical composition (concentration, ion-composition, etc.) of the liquid phase of the soil from the viewpoint of flow studies (especially in saline and/or alkali environment), some results are shown in Figure 4.22 from one of our laboratory model experiments. The flow of water and 0.05 N, 0.1 N and 0.5 N NaCl and Na_2CO_3 solutions were studied in a clay loam topsoil (No. 146) [VÁRALLYAY 1976a, 1978b].

The measured ESP values, saturated hydraulic conductivities (K = = cm/day) and the parameters of equations (4.28) and (4.29), characterizing the unsaturated conductivity – suction relationships ($k = f(\psi)$) was summarized in Table 4.12.

The data prove that unsaturated flow is strongly influenced by the chemical composition (concentration, ion-composition) of the soil solution and by the physico-chemical interactions between the solid and liquid phases.

In the studied concentration range, however, the influence of NaCl proved to be insignificant. This is in a good agreement with the well-known fact that the permeability and internal drainage conditions of soils with chloride-type salinization are generally much better than that of sulphate

and particularly soda-salinized soils [KOVDA 1947, 1965; SZABOLCS 1961, 1965, 1969, 1971b, 1974 and others].

Under the effect of increasing concentrations of Na_2CO_3 the sodium saturation (ESP) and moisture retention increased (Table 4.4, Fig. 4.7) and hydraulic conductivity decreased, especially (drastically) in saturated conditions and in the low suction range (Fig. 4.22).

The rate of k-decrease with increasing suction was moderated with increasing Na_2CO_3 concentration as can be seen in Figure 4.22. It is also reflected by the decrease of n-values in equations (4.28) and (4.29): Table 4.13. [This phenomena is an indirect proof of non-Darcian flow behaviour in heavy-textured swelling clays with high ESP: unsaturated conductivity, calculated for the *water-filled* cross-section of the soil matrix, increased as the gradient of the acting forces ($\approx$ grad ψ) increased, because an increasing part of the relatively strongly-bound pore water (which is immobile and has a special "semi-solid" character below a certain hydraulic gradient) was mobilized and took part in the flow process.]

As a consequence of this fact the influence of Na_2CO_3 solutions (e.g. sodium saturation, alkalinity) gradually decreased with increasing suction: it was only moderate in the medium suction range (pF 2.7 – 4.0), while in the high suction range (at and over pF 4.5 – 5.0) the k values of unsaturated hydraulic conductivity proved to be similar in all variants ($\approx 1 - 3 \cdot 10^{-6}$ cm/day). But here, of course, the liquid flow has negligible significance.

Consequently, in highly sodium-saturated soils the infiltration and downward flow (wet conditions, low gradient) are more limited than the upward capillary flow (dry conditions, high gradient) which helps progressive salinization and alkalization in the presence of a shallow, saline (Na_2CO_3) ground water and these unfavourable changes cannot be balanced by the traditional leaching and drainage techniques [International Source Book 1967; KOVDA 1947, 1965; PACHEPSKY and POPOVA 1972; Salinity Problems ... 1961; SZABOLCS 1965, 1969, 1971b, 1974; SZABOLCS, DARAB and VÁRALLYAY 1969, 1976; 1977, 1978b; VÁRALLYAY and SZABOLCS 1974, 1978].

Having adequate data on the above-mentioned relationships, the presented hydrophysical approach for the description and forecast of salt accumulation from the ground water can be properly improved. Using real conductivity values, corresponding to the actual concentration and ion composition of the soil solution, the natural conditions can be adequately approximated. It needs further studies and international cooperation. The various models presented in the following chapters may be of considerable help in this respect.

List of Symbols

AMR	available moisture range [volume %]
$C_{solution}$	average concentration of the filtrating soil solution [g/litre]
C_t	Cl^- concentration of the soil solution [me/litre.]
CEC	cation exchange capacity [me/100 g soil]
D	diffusivity [cm^2/day]
EC	electrical conductivity [mmhos/cm]
ESP	exchangeable sodium percentage
FC	field capacity (water storage capacity) [volume %]

FG MQ SQ	data of the analysis of variance (AOV) table
ΔH	hydraulic head at the beginning of the experiment [mm]
grad H	hydraulic gradient [cm/cm]
HC	hydraulic conductivity [cm/day]
I_θ	volume of water removed from unit volume of soil, per unit of time [cm³/sec]
IR	infiltration rate [mm/hour]
K	saturated hydraulic conductivity [cm/day]
K_0	saturated hydraulic conductivity at the beginning of the experiment [cm/day]
K_∞	saturated hydraulic conductivity at equilibrium state [cm/day]
L	length of the soil column [cm]
P_T	total porosity [in volume %]
Q	quantity of water filtrating through the soil column [cm³/day]
R	correlation coefficient
$R^2\pi$	surface area of the soil column [cm²]
S_0	standard state (reference level)
T_0	temperature [°C]
TC	total water storage capacity [in volume %]
V	flow velocity; volume of water flow through a unit cross section per unit of time in the direction of the x-axis [cm/day]
V_{salt}	net influx of salts from the ground water to the overlying horizons [t/ha/year]
V_{water}	net influx of water from the ground water to the overlying horizons [t/ha/year]
$\overline{V}_w$	partial specific volume of the constituent water in the soil solution
WP	wilting percentage [volume %]
a	experimentally determined constant in equations (4.28) and (4.29)
b	experimentally determined constant in equation (4.29)
b_0, b_1, b_2, b_3, b_4, b_5	parameters of the fifth-degree polynomial equation (partial regression coefficients)
b and c	experimentally determined parameters in equation (4.14a)
c and pF_0	experimentally determined parameters in equation (4.14b)
Δh	hydraulic head at the end of the experiment [mm]
Δh_c	constant hydraulic head [cm]
hy	hygroscopicity [weight %]
k	capillary conductivity (unsaturated hydraulic conductivity) [cm/day]
m	experimentally determined exponent in equations (4.7), (4.8), (4.9) and (4.10)
n	experimentally determined exponent in equations (4.28) and (4.29)
$r^2\pi$	surface area of the liquid-containing tube [cm²]
Δt	time interval of the measurement [days]
x	θ (moisture content in vol. %) in the fifth-degree polynomial equation

y	pF-value in the fifth-degree polynomial equation
z	height above a certain reference level (e.g. vertical distanc) from the water table) [cm]
α	experimentally determined constant in equation (4.30)
ε_ψ	experimentally determined constant in equations (4.9) and (4.10
θ	moisture content [volume percentage, θ]
θ^*	water filled pore volume [cm^3/cm^3]
θ_0	moisture content of the saturated soil [volume percentage]
μ	experimentally determined constant
π	experimentally accessible osmotic pressure of the solution
ψ	matric potential (suction)
ψ_a	suction at air entry point [water column cm]
ψ_g	gravitational potential
ψ_{max}	validity limit in equation (4.30) [water column cm]
ψ_p	tensiometer-pressure potential
ψ_p^a	pneumatic potential
ψ_s	osmotic potential
ψ_{sr}	osmotic potential in plant root tissues
ψ_{ss}	osmotic potential in soil solution
ψ_t	total soil moisture potential [J/kg]
ψ_0	experimentally determined constant in equations (4.7), (4.8,) (4.9) and (4.10)